NATIONAL ADVISORY COMMITTEE FOR AERONAUTICS

TECHNICAL NOTE 4057

INVESTIGATION AT LOW SPEEDS OF DEFLECTORS AND SPOILERS AS GUST ALLEVIATORS ON A MODEL OF THE BELL X-5 AIRPLANE WITH 35° SWEPT WINGS AND ON A HIGH-ASPECT-RATIO 35° SWEPT-WING—FUSELAGE MODEL

By Delwin R. Croom and Jarrett K. Huffman

Langley Aeronautical Laboratory
Langley Field, Va.

Washington
June 1957

NATIONAL ADVISORY COMMITTEE FOR AERONAUTICS

TECHNICAL NOTE 4057

INVESTIGATION AT LOW SPEEDS OF DEFLECTORS AND SPOILERS AS GUST ALLEVIATORS ON A MODEL OF THE BELL X-5 AIRPLANE WITH 35° SWEPT WINGS AND ON A HIGH-ASPECT-RATIO 35° SWEPT-WING—FUSELAGE MODEL

By Delwin R. Croom and Jarrett K. Huffman

SUMMARY

An investigation was made at low speeds in the Langley 300 MPH 7- by 10-foot tunnel to determine the gust-alleviation capabilities (reduction in lift-curve slope) of spoilers and deflectors on a high-aspect-ratio 35° swept-wing—fuselage model and a 1/4-scale model of the Bell X-5 airplane with 35° swept wings.

The results indicate that deflector and spoiler-deflector types of controls can be designed to provide considerable gust alleviation for a swept-wing airplane while still maintaining stability and control.

INTRODUCTION

Results reported in reference 1 showed that spoilers and deflectors, when mounted near the leading edge of the unswept wing of a transport model, were effective in reducing the normal acceleration due to gusts by reducing the lift-curve slope. It was anticipated that this type of control would be extended when rough air was encountered by a transport airplane and remain extended as long as the airplane remained in rough air. The investigation has been extended in this report to include similar devices on swept wings.

A preliminary series of tests, referred to in reference 1, was made on a wing with an aspect ratio of 8.35 and 34.9° of sweep (referred to the unswept-wing quarter-chord line). The results indicated that the devices should be placed farther back on a swept wing than on the unswept wing model of reference 1 and might require ventilation from the lower to the upper wing surface. Several of the more effective configurations found in these preliminary tests were incorporated in the investigation of the high-aspect-ratio model and the 1/4-scale model of the Bell X-5 airplane with the wings swept back 35°.

SYMBOLS

The results of the investigation are presented as standard coefficients of forces and moments about the wind axes.

C_D	drag coefficient, Drag/qS
$C_{D,b}$	drag coefficient of the basic model
C_L	lift coefficient, Lift/qS
C_m	pitching-moment coefficient, referred to $0.25\bar{c}$, $\frac{\text{Pitching moment}}{qS\bar{c}}$
C_l	rolling-moment coefficient due to control
$C_{L_{\alpha,b}}$	slope of lift curve of basic model, per deg
C_{L_α}	slope of lift curve of model with deflectors or spoilers, per deg
b	wing span, ft
b_d	deflector span, ft
c	wing chord parallel to free airstream, ft
$\bar{c}$	wing mean aerodynamic chord, ft
c_{av}	average streamwise chord spanned by control, ft
$c_{\Lambda=0^\circ}$	wing chord measured perpendicular to quarter-chord line of unswept wing, ft
q	dynamic pressure, lb/sq ft
S	wing area, sq ft
i_t	horizontal-tail incidence, positive when trailing edge is deflected down, deg
x	longitudinal distance, ft
$(x_d)_{\Lambda=0^\circ}$	chordwise position of deflector measured perpendicular to quarter-chord line of unswept wing, ft

$\frac{y_i}{b/2}$ inboard end of control, fraction of wing semispan

$\frac{y_o}{b/2}$ outboard end of control, fraction of wing semispan

α angle of attack, deg

δ_a left aileron deflection, positive when trailing edge is deflected downward, deg

δ_d deflector projection, negative direction away from chord plane, fraction of wing chord

δ_s spoiler projection, negative direction away from chord plane, fraction of wing chord

MODELS AND APPARATUS

Two models were used in the present investigation, a 1/4-scale model of the Bell X-5 research airplane having wings with 35° of sweep (referred to the unswept-wing quarter-chord line) and a wing-fuselage model having a wing with 34.93° of sweep (referred to the unswept-wing quarter-chord line). This wing-fuselage model had a taper ratio of 0.589, an aspect ratio of 8.35, and NACA 65A009 airfoil sections at an angle of 43.83° with the wing leading edge. It is hereinafter referred to as the high-aspect-ratio model. Drawings and physical characteristics of the models are shown in figure 1. The high-aspect-ratio model and the X-5 model were tested with various combinations of spoilers and deflectors. The various control spans, chordwise locations, and projections are given in table I and figures 1(b) and 2. Ventilation through the wing for the spoiler-slot-deflectors and for the butterfly-valve arrangements on the X-5 model was accomplished by drilling 22 holes, 13/16 inch in diameter and spaced with centers $1\frac{1}{8}$ inch apart, along the $0.35c_{\Lambda=0°}$ line between 0.34b/2 and 0.84b/2. (See fig. 2.) The butterfly-valve arrangement consisted of circular disks that closed the holes in the neutral condition and when deflected 90° formed a scalloped spoiler with a projection of $2\frac{1}{2}$ percent on the upper surface of the wing. Ventilation through the wing for the spoiler-slot-deflector on the high-aspect-ratio model was accomplished by means of a $0.097c_{\Lambda=0°}$ slot along the $0.143c_{\Lambda=0°}$, $0.386c_{\Lambda=0°}$, and $0.637c_{\Lambda=0°}$ lines between 0.29b/2 and 0.49b/2. (See fig. 1(b).)

The static longitudinal and lateral aerodynamic characteristics of the models were obtained on the single-strut support system in the Langley 300 MPH 7- by 10-foot tunnel.

TESTS

The tests on the high-aspect-ratio model were made at a dynamic pressure of approximately 34.5 pounds per square foot, which corresponds to an airspeed of about 170 feet per second, and the tests on the X-5 model were made at a dynamic pressure of approximately 44.5 pounds per square foot, which corresponds to an airspeed of about 193 feet per second. Reynolds number for these airspeeds, based on the wing mean aerodynamic chords of the models, are approximately 0.94×10^6 and 1.89×10^6 for the high-aspect-ratio model and X-5 model, respectively. The various configurations tested are listed in table I.

CORRECTIONS

The values for angle of attack and drag have been corrected for jet-boundary effects by the method of reference 2. The data have been corrected for tunnel air-flow misalinement, tunnel blockage, and longitudinal pressure gradient in the tunnel.

RESULTS AND DISCUSSION

Summary plots which show the effect of chordwise location, projection, and span of the various spoiler and deflector configurations on the gust-alleviation capabilities (reduction in lift-curve slope) are presented in figures 3 to 5. The solid symbols in these figures indicate that the variation of lift with angle of attack was nonlinear, as shown in the basic-data figures (figs. 6 to 25) from which these points were obtained.

The ratios of the lift-curve slopes of the models with controls to the lift-curve slopes of the basic models are presented in figure 3 as a function of the chordwise location of the controls for several control configurations on the X-5 model and the high-aspect-ratio model. It is indicated in figure 3 that these controls became more effective in reducing the lift-curve slope as they were moved rearward to approximately the 35-percent-chord line. The maximum reduction was obtained for these models when the controls were located between the 25- and 35-percent-chord lines. On the unswept-wing model of reference 1 the controls were located along the 12-percent-chord line and gave 20- to

40-percent reductions in lift-curve slope. The results of the present investigation and that of reference 1 indicate that the controls should be located farther back on a swept wing than on an unswept wing in order to obtain the desired reduction in lift-curve slope.

The magnitudes of the reductions in lift-curve slope achieved with the devices which extended from 0.34b/2 to 0.84b/2 are shown in figure 4(a), where the lift-curve-slope ratio is plotted against deflector projection for the several devices. The deflector alone gave reductions up to about 35 percent for a deflector projection of 15 percent of the wing chord. If more reduction than this is desired, ventilation through the wing is required. A spoiler-slot-deflector with a spoiler projection of $2\frac{1}{2}$ percent of the wing chord (the optimum projection for this arrangement) gives a reduction of about 50 percent for a 15-percent projection of the deflector. Since the spoiler-slot-deflectors appear to provide more reduction in lift-curve slope than the plain deflectors, two variations of the spoiler of the basic spoiler-slot-deflector were studied. One was a spoiler that was sufficiently long to cover the holes and was deflected to $2\frac{1}{2}$ percent of the wing chord (hereafter in this report referred to as the slant spoiler), and the other was a butterfly-valve arrangement. Both these arrangements provided larger reductions in lift-curve slope than the basic spoiler-slot-deflector. When the deflector was projected 15 percent of the wing chord, the slant-spoiler arrangement reduced the lift-curve slope about 62 percent and the butterfly-valve arrangement reduced the lift-curve slope about 70 percent, which was the maximum reduction attained for the 50-percent-span controls. (See fig. 4(a).)

The plain-deflector, spoiler-slot-deflector, slant-spoiler, and butterfly-valve arrangements were also tested with a shorter span (0.34b/2 to 0.66b/2) and the results are summarized in figure 4(b). The same general trends in lift-curve-slope reduction were noted for the 32-percent-span controls (fig. 4(b)) as for the 50-percent-span controls (fig. 4(a)). However, generally, the effectiveness of the control was not proportional to the span of the control.

Figures 4(a) and 4(b) also show the increase in drag resulting from the projection of the devices. It can be seen that for any of the devices that give more than 20-percent reduction in lift-curve slope, the drag ratio $\left(\text{at } C_L = 0.3\right)$ is greater than 2, which indicates that any of these devices should be good aerodynamic brakes and would aid in slowdown.

A deflector and a butterfly-valve arrangement having several spans were tested on the X-5 model to determine the effect of span of control on lift-curve-slope reduction. These data are presented in figure 5.

The inboard ends of these controls were at 0.34b/2 except for the 18-percent-span controls, which began at 0.41b/2. It can be seen from these data that when the deflector was located along the 35-percent-chord line the reduction in lift-curve slope did not decrease with decreased span of control as rapidly as when the deflector was located along the 25-percent-chord line. It may also be seen that for the 35-percent-chord location the lift curve was linear, whereas for the 25-percent-chord location the lift curve was nonlinear.

Figure 6 shows the effect of spoiler projection on the linearity of the lift curve of a typical spoiler-slot-deflector arrangement on the X-5 model. In order to obtain linear or near linear lift curves the correct ratio of spoiler projection to deflector projection must be determined for each installation. For the X-5, figure 6 indicates that $\frac{\delta_d}{\delta_s} = \frac{-0.025}{-0.15}$ resulted in a linear lift curve. The effect, if any, that nonlinear lift curves have on the gust-alleviation capabilities has not been determined.

The effect of ventilation from lower to upper surface on the lift curve is shown in figure 7. As the ventilation is increased, at least up to the maximum used for these tests, the reduction in lift-curve slope becomes larger.

The longitudinal stability characteristics of the X-5 model with a butterfly-valve arrangement are presented in figure 8 for two spans. It can be seen that the control with the longer span had a destabilizing effect on the pitching moment, whereas the control with the shorter span was more stable than the plain wing configuration up to a lift coefficient of 0.70. These results indicate the problems that may be encountered with some wings. The longitudinal aerodynamic characteristics of all the control configurations are presented in figures 9 to 25.

The effects of the devices on the lateral control characteristics of the X-5 model are shown in figure 26, where the rolling-moment coefficient due to $\pm 10^\circ$ of aileron deflection is plotted against angle of attack for the wing equipped with a butterfly-valve or a spoiler-slot-deflector arrangement. The inboard end of the aileron was at 0.66b/2, and when the devices extended outboard of this point (from 0.34b/2 to 0.84b/2), the aileron was ineffective in the low and moderate angle-of-attack range. However, when the devices were located entirely inboard of the aileron (from 0.34b/2 to 0.66b/2), aileron control was maintained throughout the moderate angle-of-attack range and the aileron had more than 50 percent of the effectiveness of the aileron on the plain-wing configuration.

Since these spoiler-slot-deflector devices resemble a spoiler-slot-deflector type of aileron, a few tests were made to evaluate such a

device for use as both an aileron and a gust alleviator. These data are presented in figure 27. As shown by the sketches in figure 27, for the condition with the gust-alleviation device retracted the linkages are so arranged as to project the spoiler 15 percent and the deflector 5 percent of the wing chord to obtain lateral control. For the condition with the gust-alleviation device extended the spoiler is projected $2\frac{1}{2}$ percent and the deflector 10 percent, and to obtain lateral control the spoiler projection is increased to 15 percent on the left wing. It can be seen that for both the retracted and extended conditions, for both spans of the controls (0.34b/2 to 0.66b/2 and 0.34b/2 to 0.84b/2), this type of lateral-control device provided control as good as or better than that of the conventional aileron for $\pm 10^{\circ}$ deflection.

CONCLUDING REMARKS

The results of an investigation made at low speeds in the Langley 300 MPH 7- by 10-foot tunnel of a 35° swept-wing model of high aspect ratio and a 1/4-scale model of the Bell X-5 airplane having 35° swept wings indicate that deflector and spoiler-deflector types of controls can be designed to provide considerable gust alleviation (reduction in lift-curve slope) for a swept-wing airplane while still maintaining stability and control.

Langley Aeronautical Laboratory,
National Advisory Committee for Aeronautics,
Langley Field, Va., April 22, 1957.

REFERENCES

1. Croom, Delwin R., Shufflebarger, C. C., and Huffman, Jarrett K.: An Investigation of Forward-Located Fixed Spoilers and Deflectors as Gust Alleviators on an Unswept-Wing Model. NACA TN 3705, 1956.

2. Gillis, Clarence L., Polhamus, Edward C., and Gray, Joseph L., Jr.: Charts for Determining Jet-Boundary Corrections for Complete Models in 7- by 10-Foot Closed Rectangular Wind Tunnels. NACA WR L-123, 1945. (Formerly NACA ARR L5G31.)

TABLE I.- TYPE, PROJECTION, CHORDWISE LOCATION, AND SPAN OF THE VARIOUS CONTROLS

(a) Longitudinal data for Bell X-5 model

Type of control	δ_d, percent c_{av}	δ_s, percent c_{av}	$\frac{(x_d)_{\Lambda=0^\circ}}{c_{\Lambda=0^\circ}}$	$\frac{y_i}{b/2}$	$\frac{y_o}{b/2}$	i_t, deg	Figures
Effect of chordwise location							
Deflector	-7.5	0	0, 0.12, 0.15, 0.25, 0.40	0.34	0.91	-3/4	3 and 9
Deflector	-15.0	0	0.15, 0.25	.34	.91	-3/4	3 and 10
Deflector	-15.0	0	0.25, 0.40	.34	.91	-5	3 and 10
Effect of configuration							
Deflector	-2.5, -5.0, -7.5, -10.0, -15.0	0	0.35	0.34	0.84	-5	4(a) and 13
Spoiler-slot-deflector	-5.0, -7.5, -10.0, -15.0	-2.5	[a].35	.34	.84	-5	4(a) and 14
Slant spoiler-slot-deflector	-7.5, -10.0, -15.0	-2.5	[a].35	.34	.84	-5	4(a) and 15
Butterfly-valve arrangement	-5.0, -7.5, -10.0, -15.0	-2.5	[a].35	.34	.84	-5	4(a), 8, and 16
Deflector	-5.0, -7.5, -10.0, -15.0	0	.35	.34	.66	-5	4(b) and 17
Spoiler-slot-deflector	-5.0, -7.5, -10.0, -15.0	-2.5	[a].35	.34	.66	-5	4(b) and 18
Slant spoiler-slot-deflector	-5.0, -7.5, -10.0, -15.0	-2.5	[a].35	.34	.66	-5	4(b) and 19
Butterfly-valve arrangement	-5.0, -7.5, -10.0, -15.0	-2.5	[a].35	.34	.66	-5	4(b), 8, and 20
Effect of span							
Deflector	-15.0	0	0.25	0.34	0.50	-3/4	5 and 21
Deflector	-15.0	0	.25	.34	.70	-3/4	5 and 21
Deflector	-15.0	0	.25	.34	.91	-3/4	5 and 21
Deflector	-15.0	0	.35	.34	.66	-5	5 and 22
Deflector	-15.0	0	.35	.34	.84	-5	5 and 22
Deflector	-15.0	0	.35	.41	.59	-5	5 and 22
Butterfly-valve arrangement	-15.0	-2.5	[a].35	.34	.66	-5	5 and 23
Butterfly-valve arrangement	-15.0	-2.5	[a].35	.34	.84	-5	5 and 23
Butterfly-valve arrangement	-15.0	-2.5	[a].35	.41	.59	-5	5 and 23
Effect of spoiler-deflector ratio							
Spoiler-slot-deflector	-15.0	-2.5, -5.0, -7.5, -10.0, -15.0	[a]0.35	0.34	0.84	-5	6 and 24
Effect of ventilation							
Deflector	-10.0	Off	[a]0.35	0.34	0.84	-5	7 and 25

(b) Longitudinal data for high-aspect-ratio model

Type of control	δ_d, percent c	δ_s, percent c	$\frac{(x_d)_{\Lambda=0^\circ}}{c_{\Lambda=0^\circ}}$	$\frac{y_i}{b/2}$	$\frac{y_o}{b/2}$	i_t, deg	Figures
Effect of chordwise location							
Deflector	-15.0	0	0.114, 0.239, 0.386, 0.536	0.29	0.96	Tail off	3 and 11
Spoiler-slot-deflector	-7.5	-7.5	[a]0.143, [a]0.386, [a]0.637	.29	.49	Tail off	3 and 12

(c) Lateral data for Bell X-5 model

Type of control	δ_d, percent c_{av}		δ_s, percent c_{av}		$\frac{(x_d)_{\Lambda=0^\circ}}{c_{\Lambda=0^\circ}}$	$\frac{y_i}{b/2}$	$\frac{y_o}{b/2}$	i_t, deg	δ_a, deg	Figures
	Left wing	Right wing	Left wing	Right wing						
Basic model	-----	-----	-----	-----	-----	---	---	-5	±10	26 and 27
Butterfly-valve arrangement	-5.0	-5.0	-2.5	-2.5	[a]0.35	0.34	0.84	-5	±10	26
Butterfly-valve arrangement	-5.0	-5.0	-2.5	-2.5	[a].35	.34	.66	-5	±10	26
Spoiler-slot-deflector	-15.0	-15.0	-2.5	-2.5	[a].35	.34	.84	-5	±10	26
Spoiler-slot-deflector	-15.0	-15.0	-2.5	-2.5	[a].35	.34	.66	-5	±10	26
Spoiler-slot-deflector	-10.0	-10.0	-15.0	-2.5	[a].35	.34	.66	-5	0	27
Spoiler-slot-deflector	-10.0	-10.0	-15.0	-2.5	[a].35	.34	.84	-5	0	27
Spoiler-slot-deflector	-5.0	0	-15.0	0	[a].35	.34	.66	-5	0	27
Spoiler-slot-deflector	-5.0	0	-15.0	0	[a].35	.34	.84	-5	0	27

[a]Chordwise position of control is given as the center of the ventilating holes.

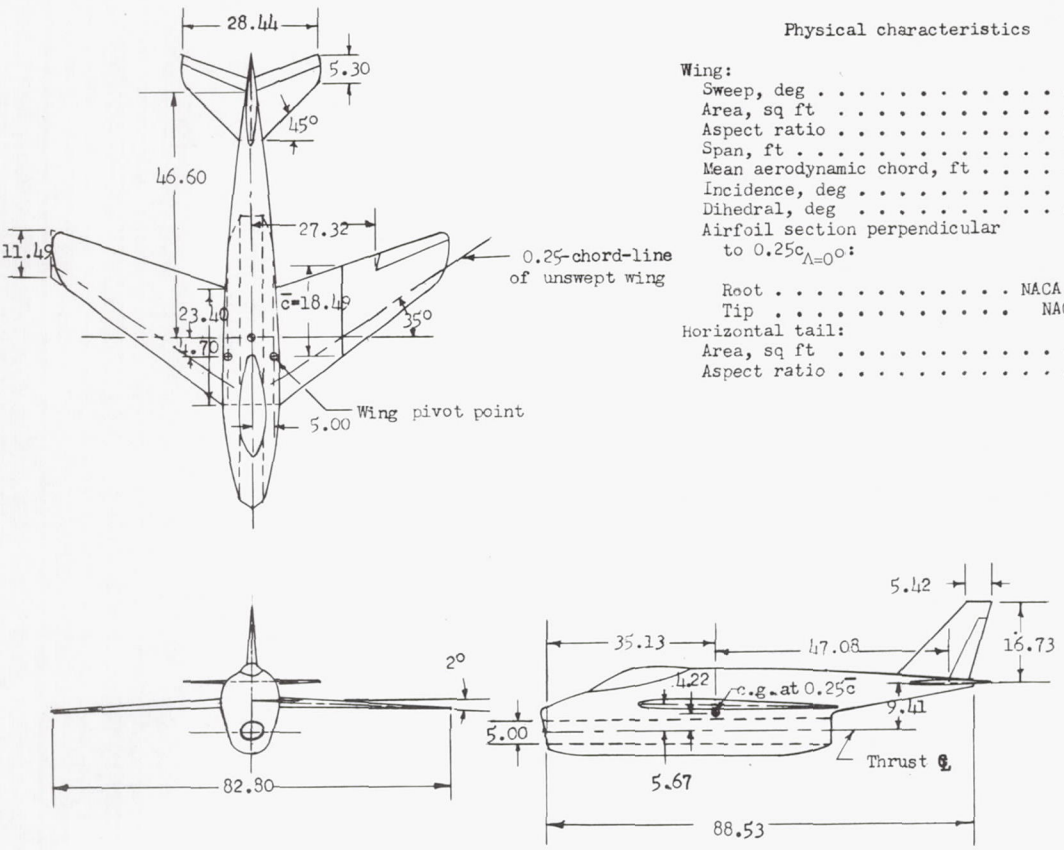

Physical characteristics

Wing:	
Sweep, deg	35
Area, sq ft	10.45
Aspect ratio	4.56
Span, ft	6.90
Mean aerodynamic chord, ft	1.579
Incidence, deg	0
Dihedral, deg	-2
Airfoil section perpendicular to $0.25c_{\Lambda=0^\circ}$:	
Root	NACA 64-010.3
Tip	NACA 64-008
Horizontal tail:	
Area, sq ft	1.94
Aspect ratio	2.89

(a) 1/4-scale model of the Bell X-5 airplane.

Figure 1.- General arrangement of the models. (All dimensions are in inches unless otherwise noted.)

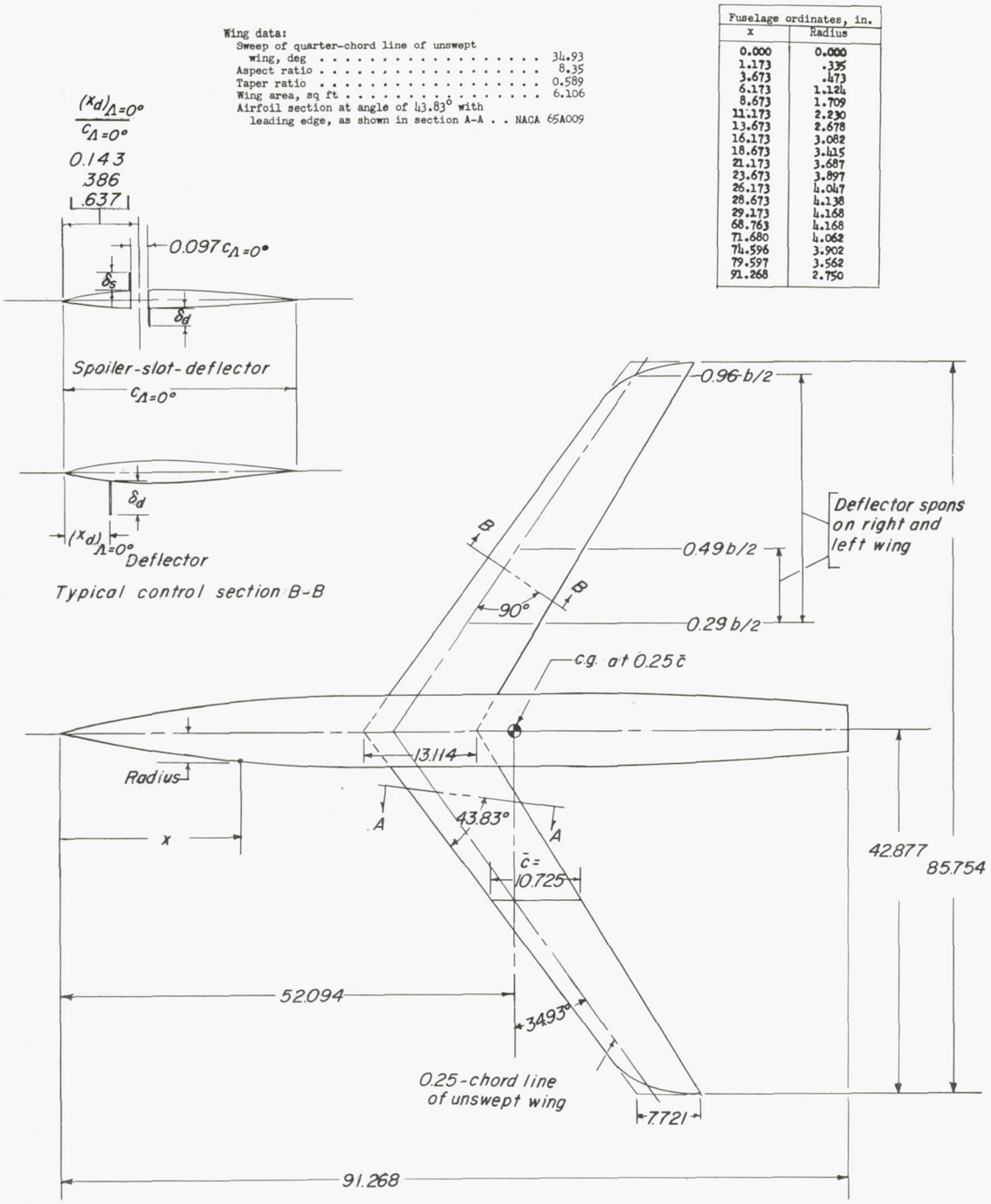

(b) High-aspect-ratio model.

Figure 1.- Concluded.

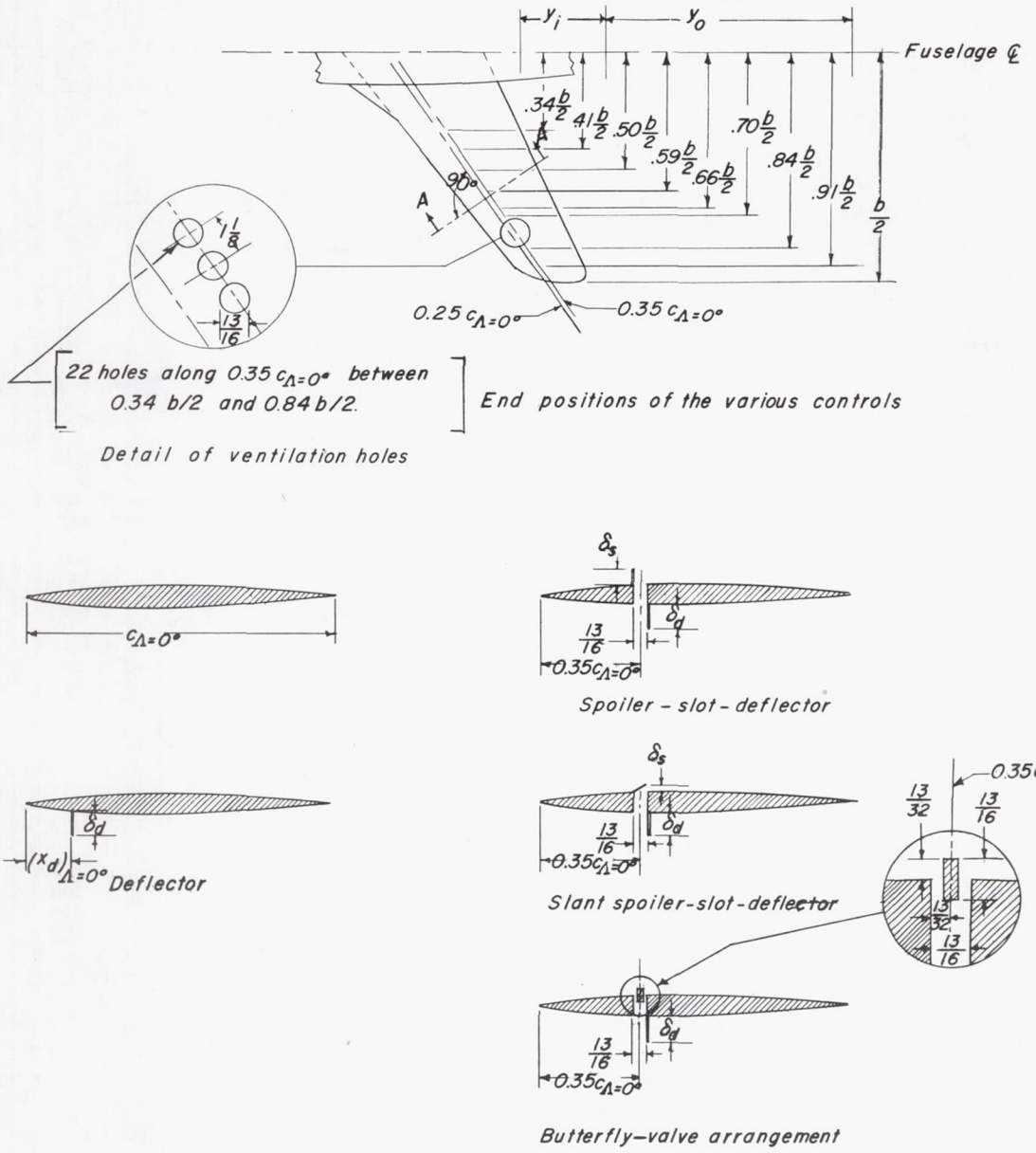

Figure 2.- Detail of controls on the 1/4-scale model of the Bell X-5 airplane. (All dimensions are in inches unless otherwise noted.)

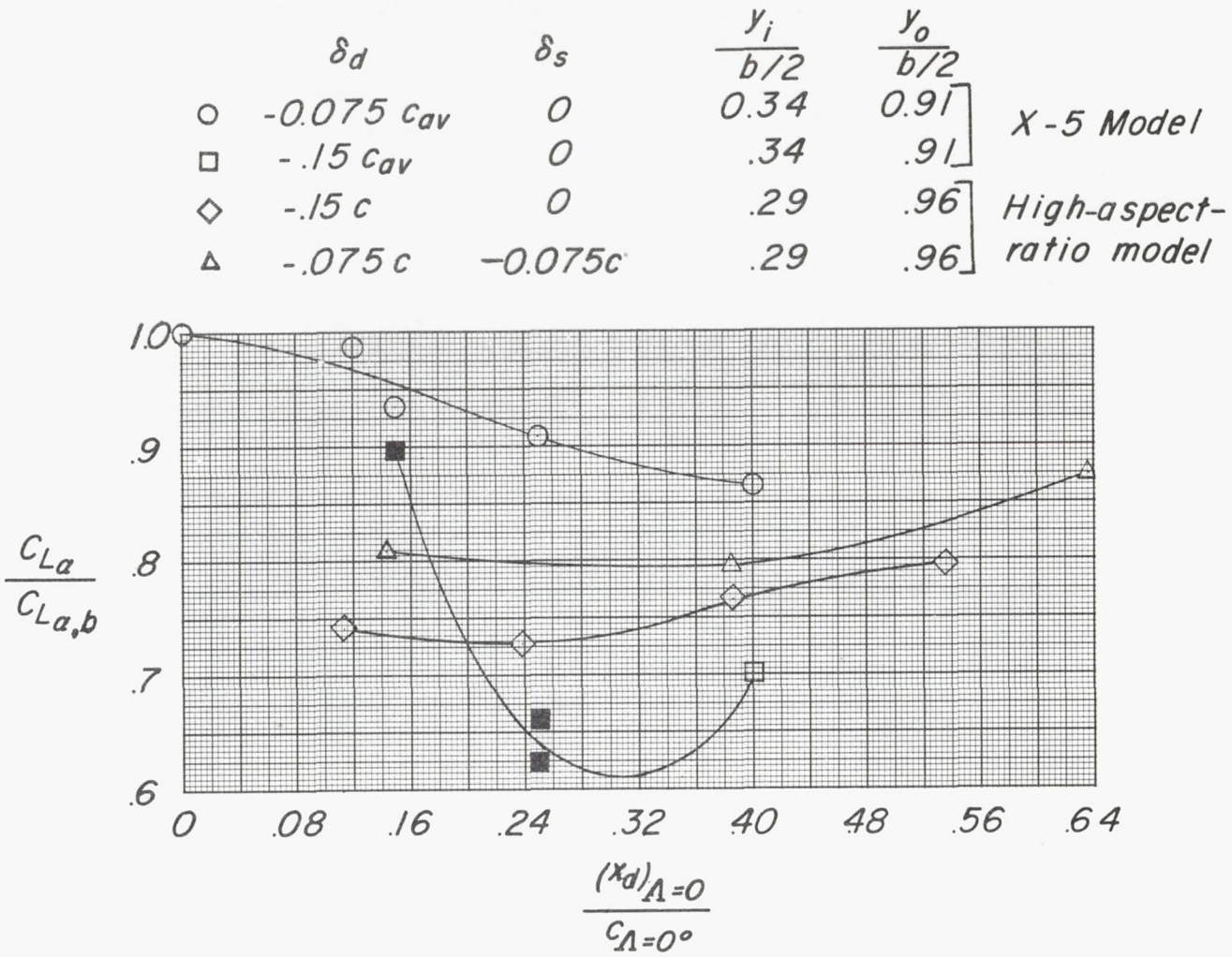

Figure 3.- Variation of lift-curve-slope reduction with chordwise location for deflector on the 1/4-scale model of the X-5 airplane and for deflector and spoiler-slot-deflector on the high-aspect-ratio model. Solid symbols indicate nonlinear lift curves.

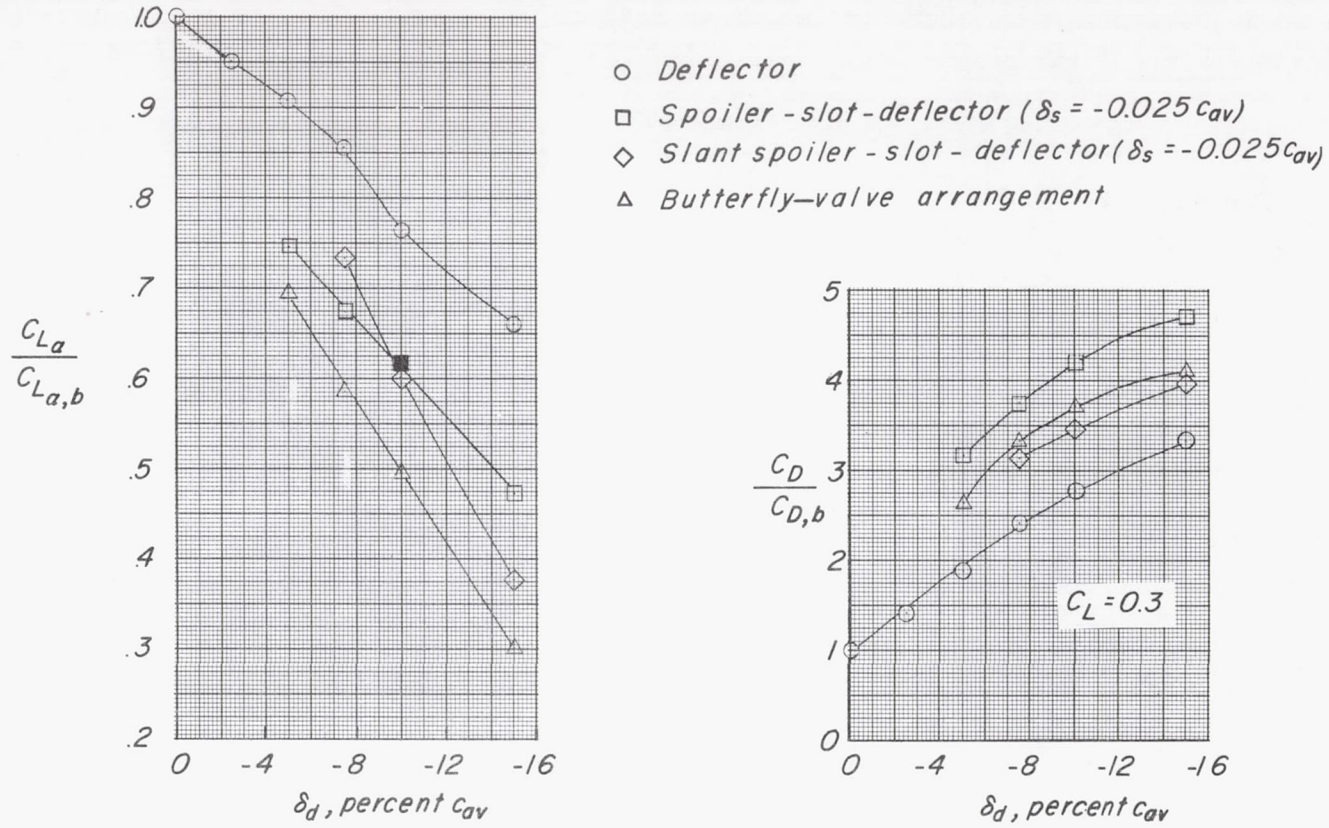

(a) $\frac{y_i}{b/2} = 0.34$; $\frac{y_o}{b/2} = 0.84$.

Figure 4.- Variation of lift-curve-slope reduction and drag increase with deflector projection for the deflector, spoiler-slot-deflector, slant spoiler-slot-deflector, and butterfly-valve arrangement on the X-5 model. $\frac{(x_d)_{\Lambda=0^\circ}}{c_{\Lambda=0^\circ}} = 0.35$; $i_t = -5^\circ$. Solid symbols indicate nonlinear lift curves.

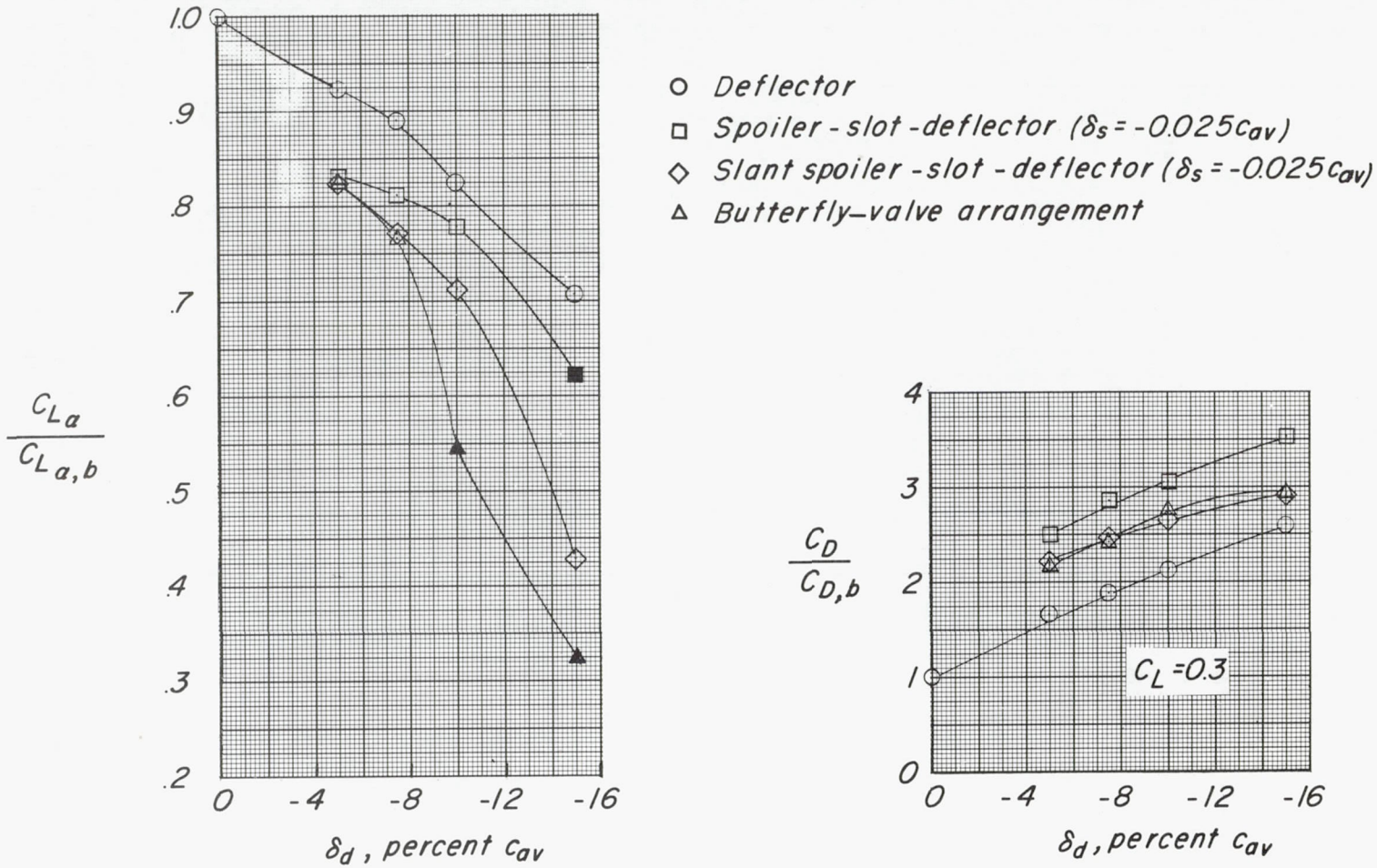

(b) $\frac{y_i}{b/2} = 0.34$; $\frac{y_o}{b/2} = 0.66$.

Figure 4.- Concluded.

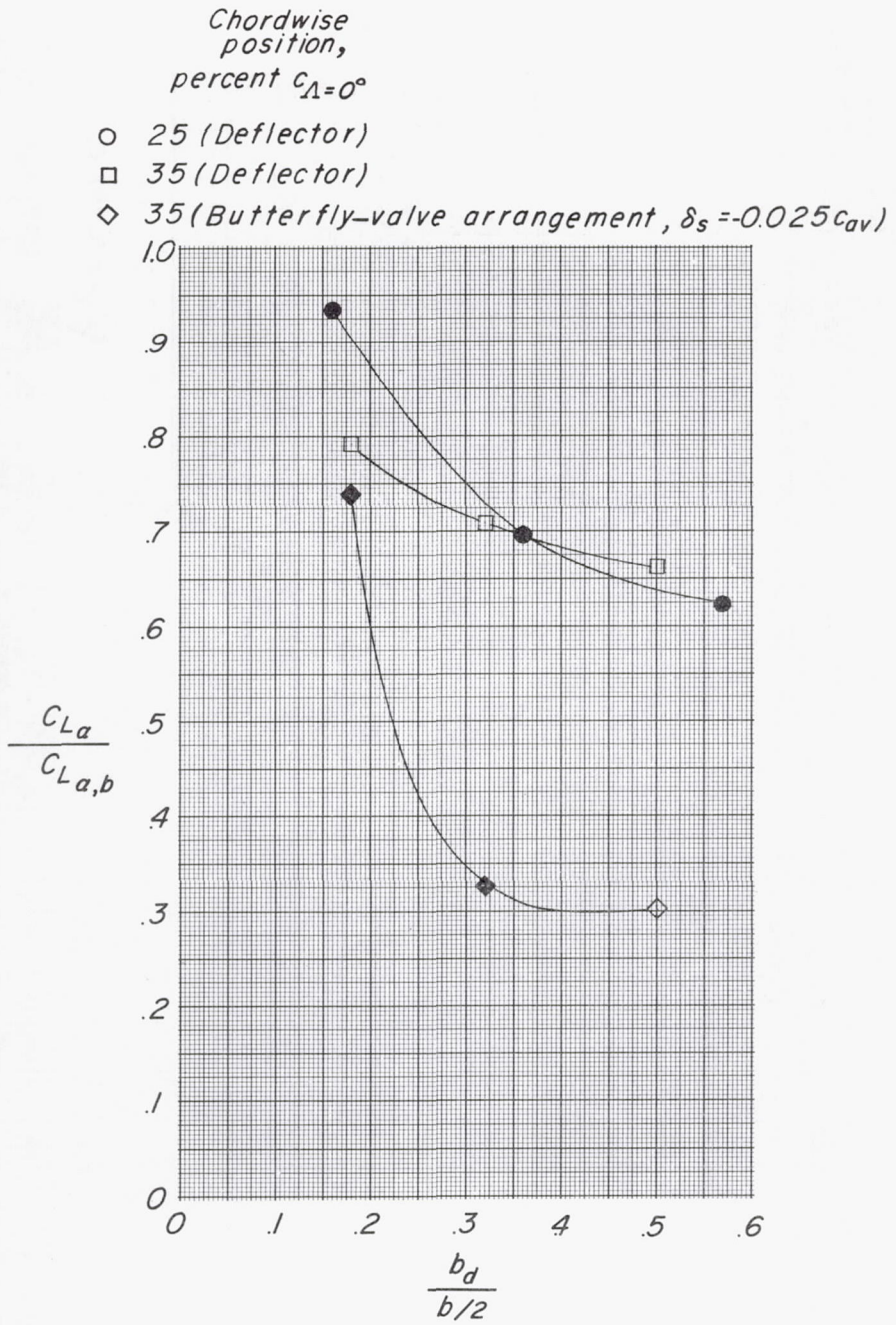

Figure 5.- Variation of lift-curve-slope reduction with span of deflector at the 25- and 35-percent-chord locations and of the butterfly-valve arrangement at the 35-percent-chord location on the 1/4-scale model of the X-5 airplane. $\delta_d = -0.15c_{av}$. Solid symbols indicate nonlinear lift curves.

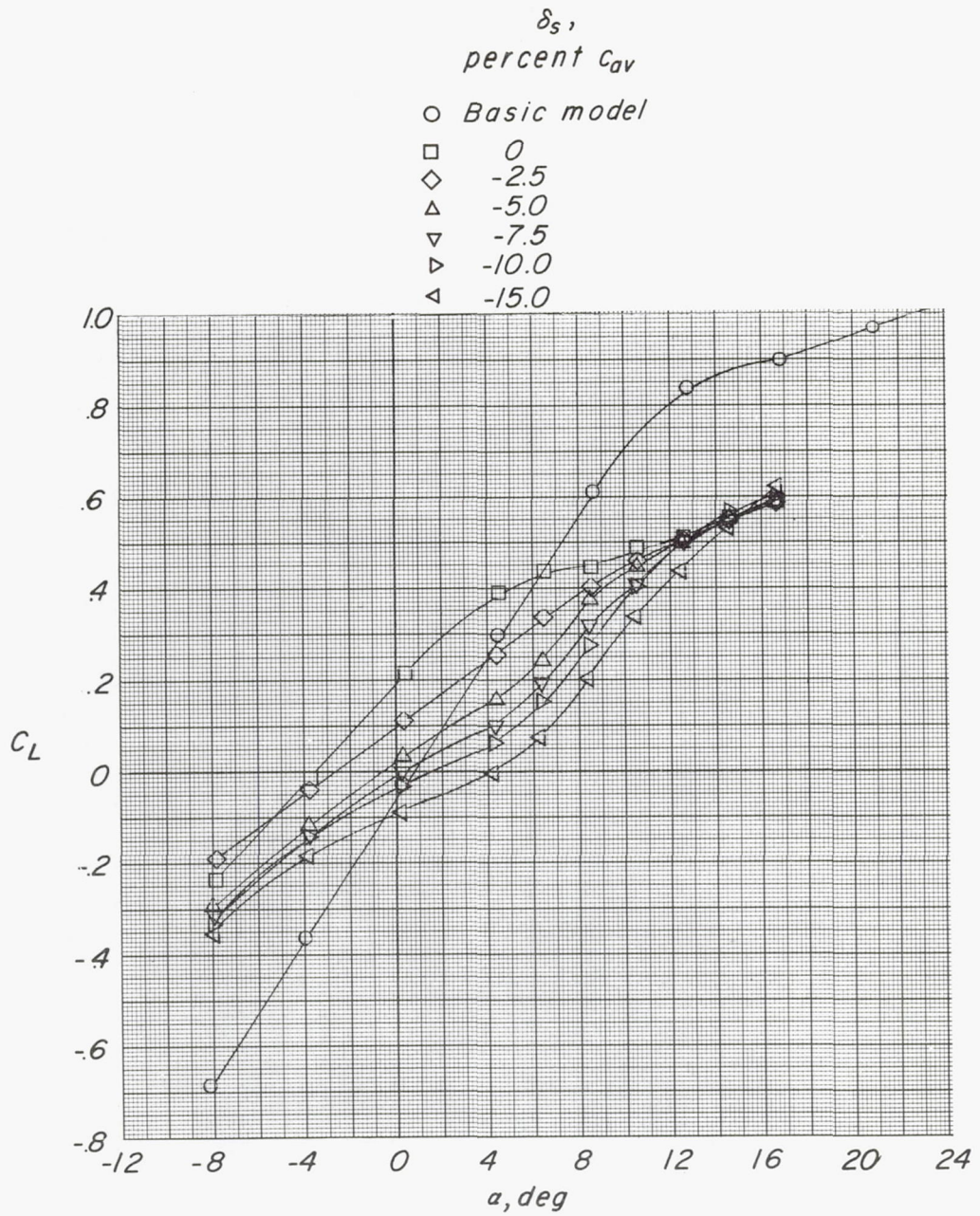

Figure 6.- Effect of spoiler projection on the linearity of the lift curve of the 1/4-scale model of the X-5 airplane with a spoiler-slot-deflector. $\delta_d = -0.15c_{av}$; $\frac{(x_d)_{\Lambda=0^\circ}}{c_{\Lambda=0^\circ}} = 0.35$; $\frac{y_i}{b/2} = 0.34$; $\frac{y_o}{b/2} = 0.84$; $i_t = -5^\circ$.

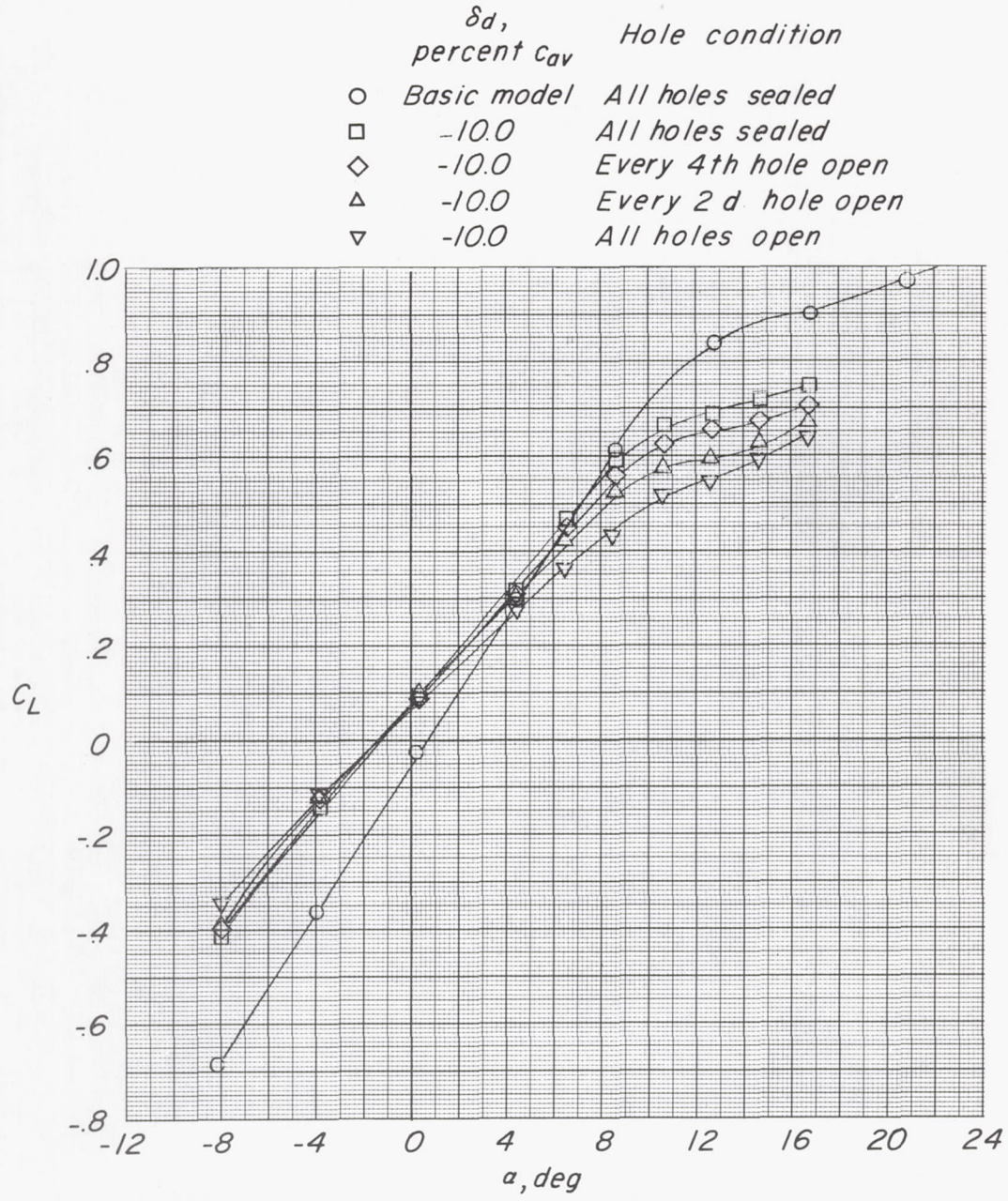

Figure 7.- Effect of ventilation on the lift-curve slope of the 1/4-scale model of the X-5 airplane with deflector. $\frac{(x_d)_{\Lambda=0^\circ}}{c_{\Lambda=0^\circ}} = 3.5$; $\frac{y_i}{b/2} = 0.34$; $\frac{y_o}{b/2} = 0.84$; $i_t = -5^\circ$.

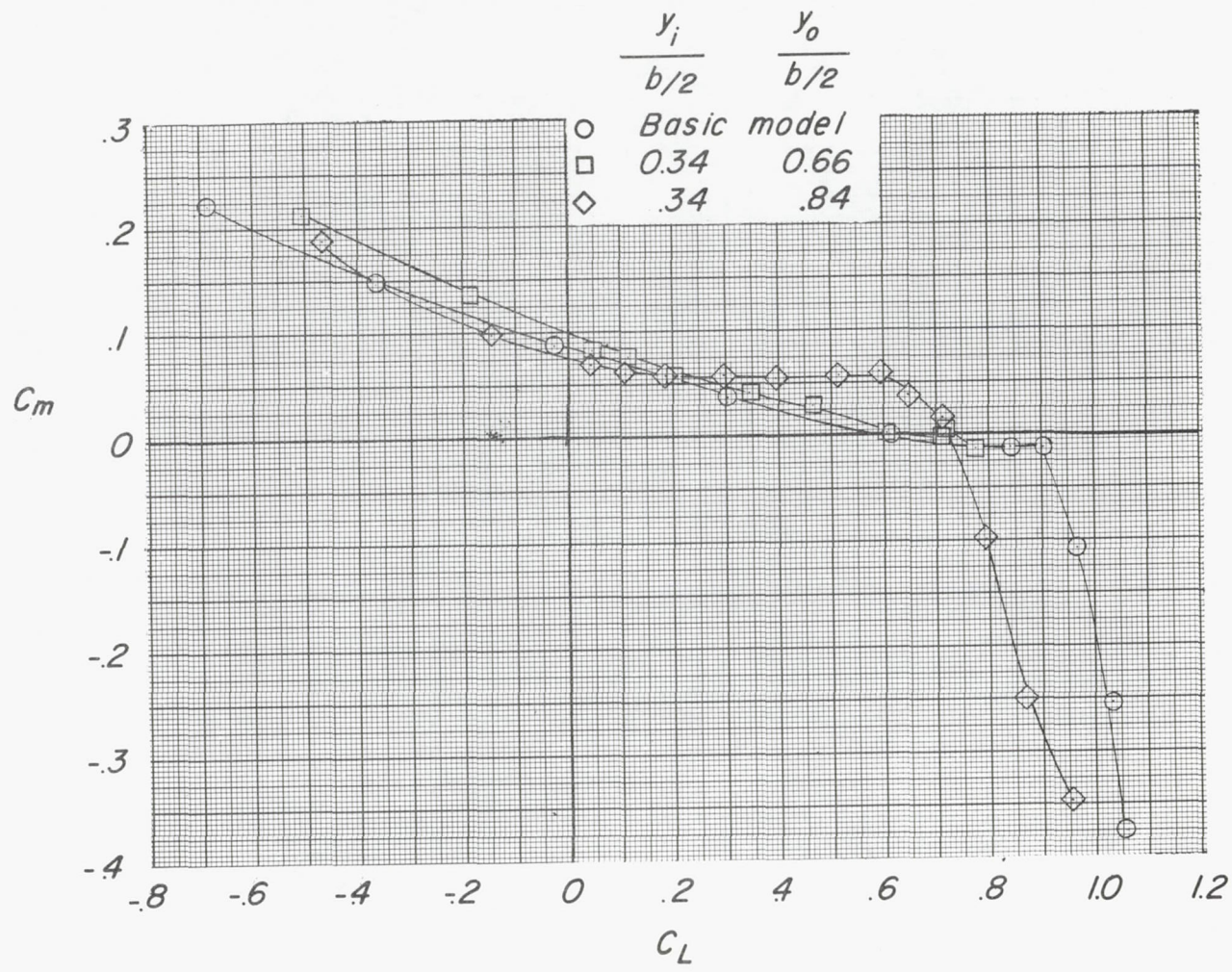

Figure 8.- Effect of span of butterfly-valve arrangement on the longitudinal stability of the X-5 model. $\delta_s = -0.025c_{av}$; $\delta_d = -0.075c$; $\frac{(x_d)_{\Lambda=0^\circ}}{c_{\Lambda=0^\circ}} = 0.35$; $i_t = -5^\circ$.

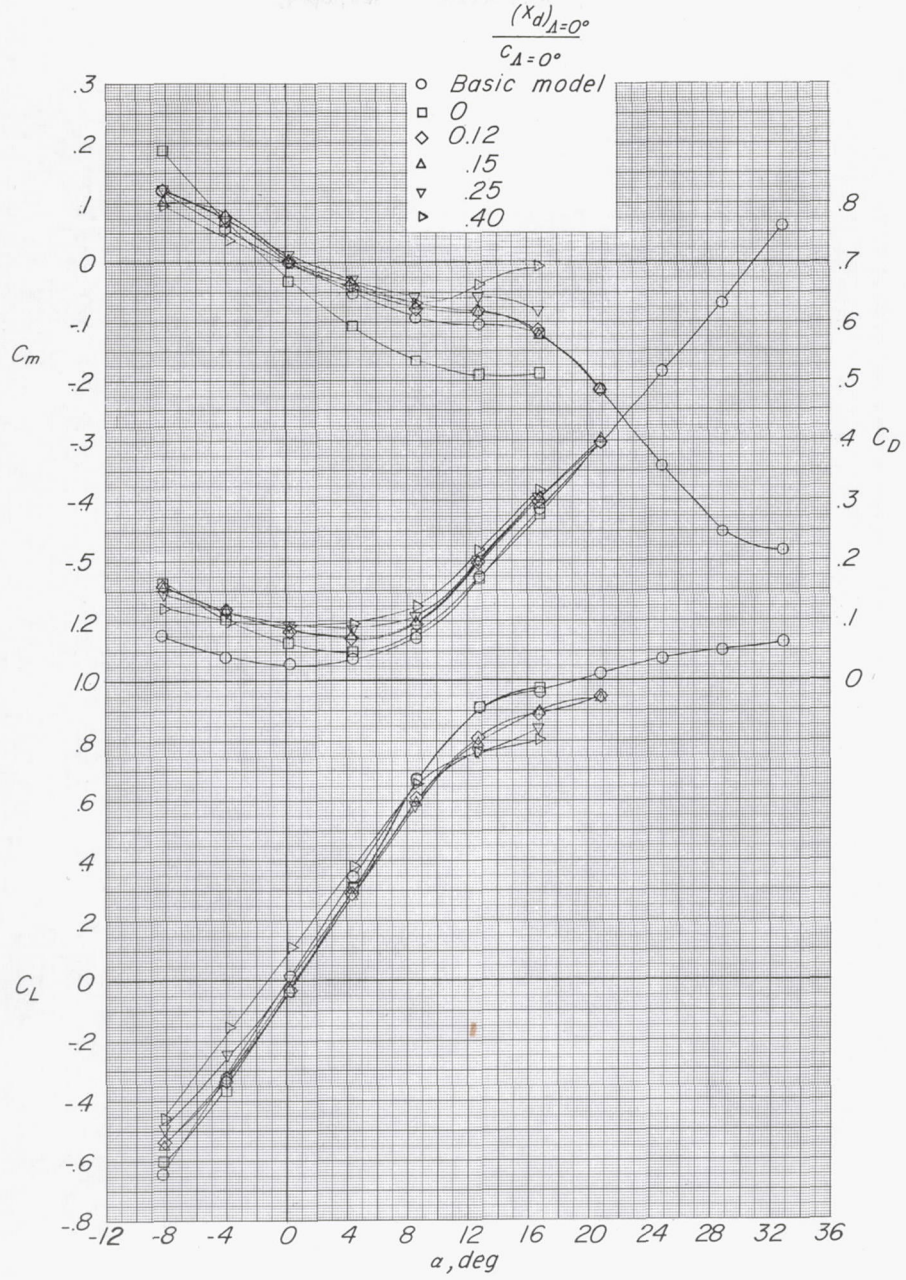

Figure 9.- Longitudinal aerodynamic characteristics of the 1/4-scale model of the X-5 airplane with deflectors. $\delta_d = -0.075c_{av}$; $\frac{y_i}{b/2} = 0.34$; $\frac{y_o}{b/2} = 0.91$; $i_t = -3/4°$.

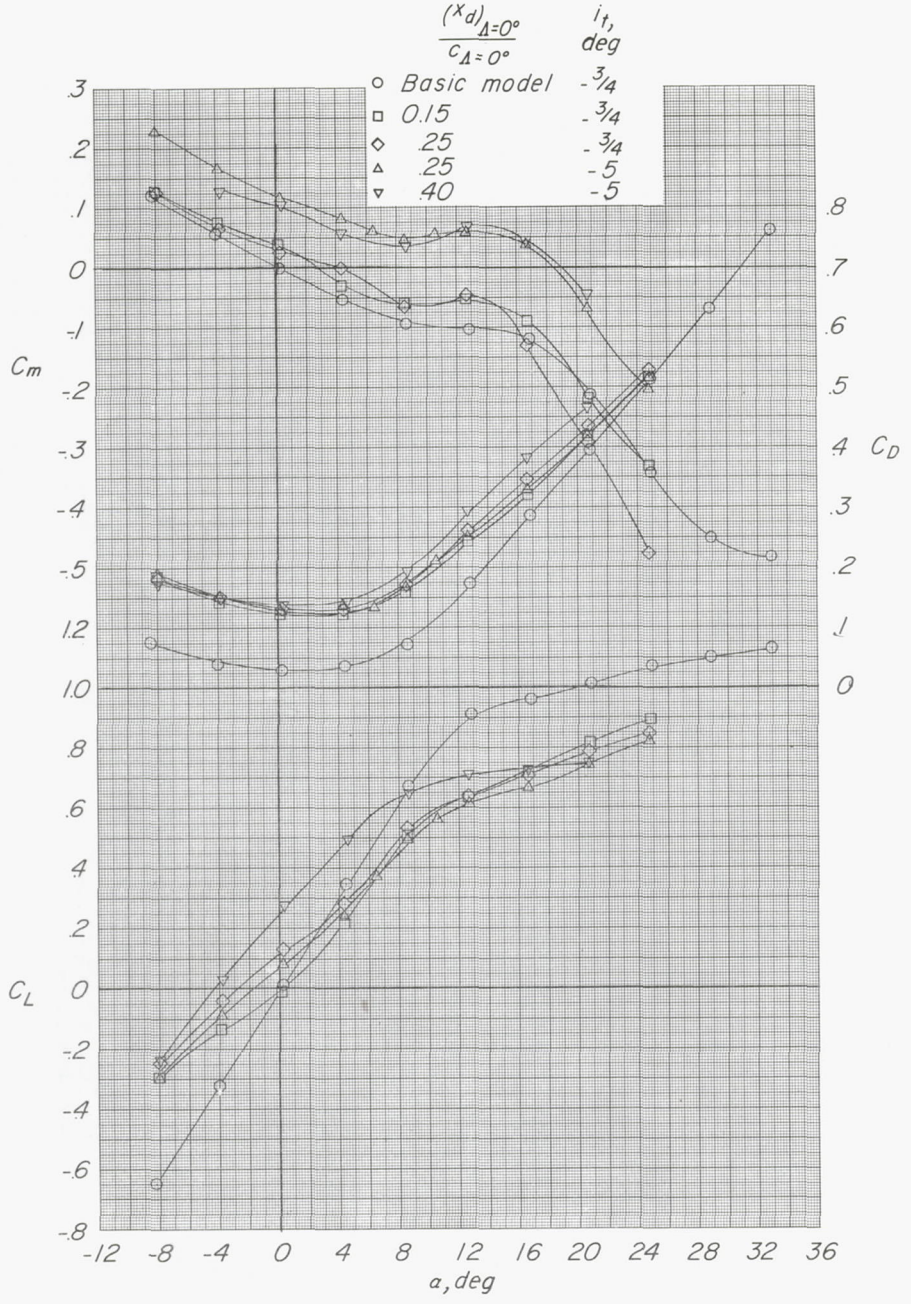

Figure 10.- Longitudinal aerodynamic characteristics of the 1/4-scale model of the X-5 airplane with deflectors. $\delta_d = -0.15c_{av}$; $\frac{y_i}{b/2} = 0.34$; $\frac{y_o}{b/2} = 0.91$.

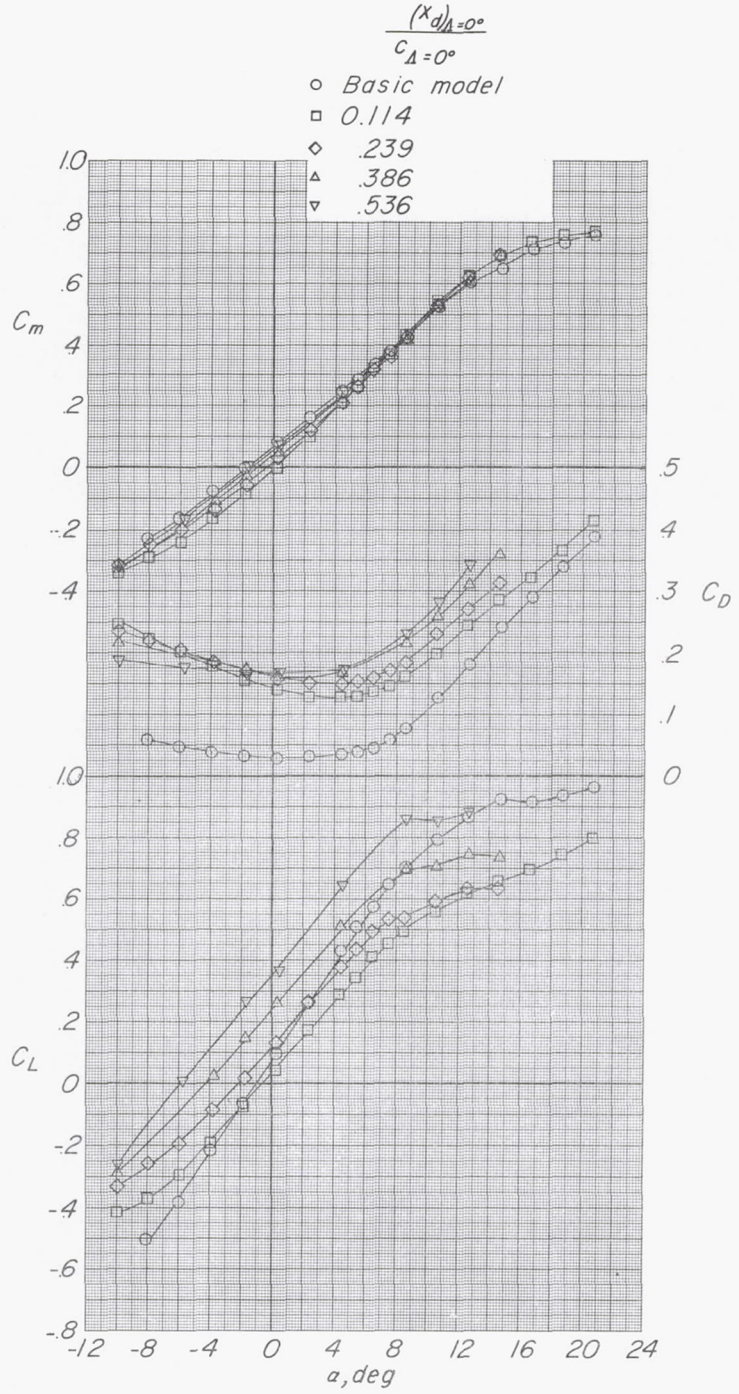

Figure 11.- Longitudinal aerodynamic characteristics of the high-aspect-ratio model with deflectors. δ_d = -0.15c; $\frac{y_i}{b/2}$ = 0.29; $\frac{y_o}{b/2}$ = 0.96.

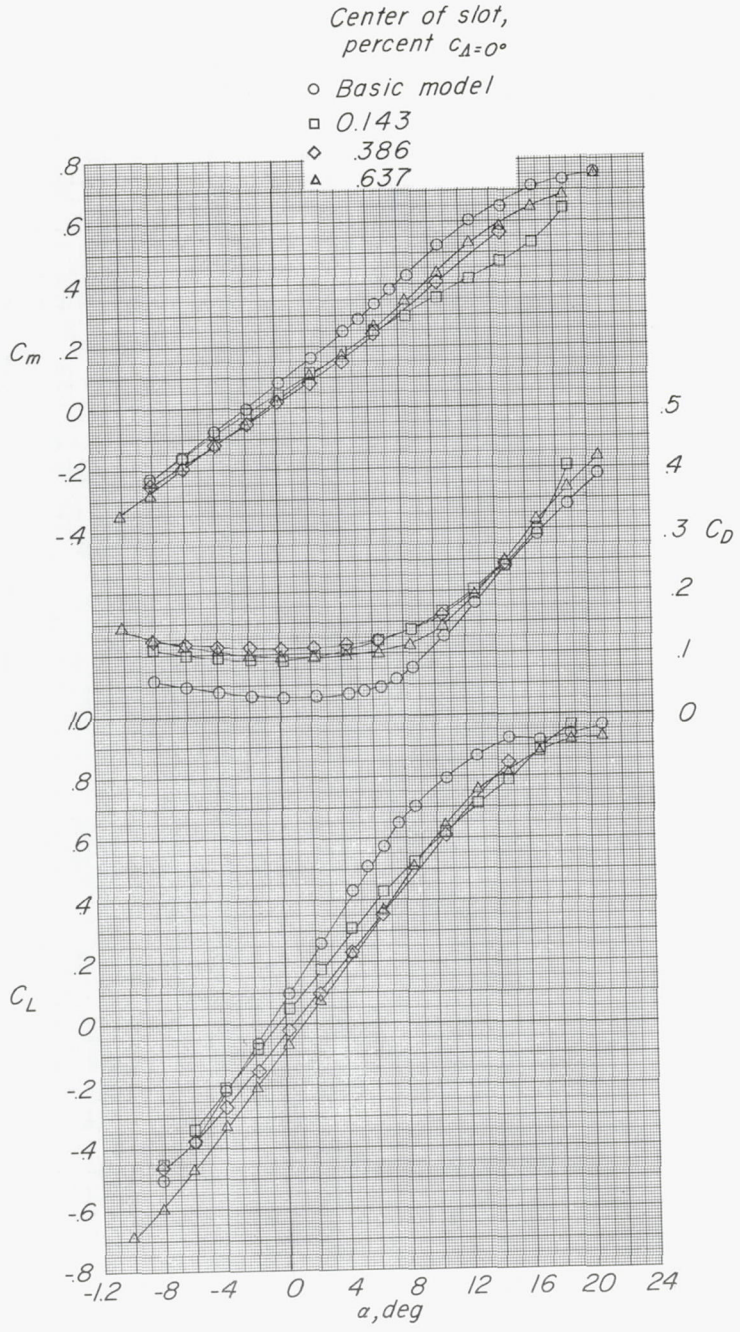

Figure 12.- Longitudinal aerodynamic characteristics of the high-aspect-ratio model with spoiler-slot-deflector. δ_d = -0.075c; δ_s = -0.075c; $\frac{y_i}{b/2}$ = 0.29; $\frac{y_o}{b/2}$ = 0.49; slot width, $0.097c_{\Lambda=0°}$.

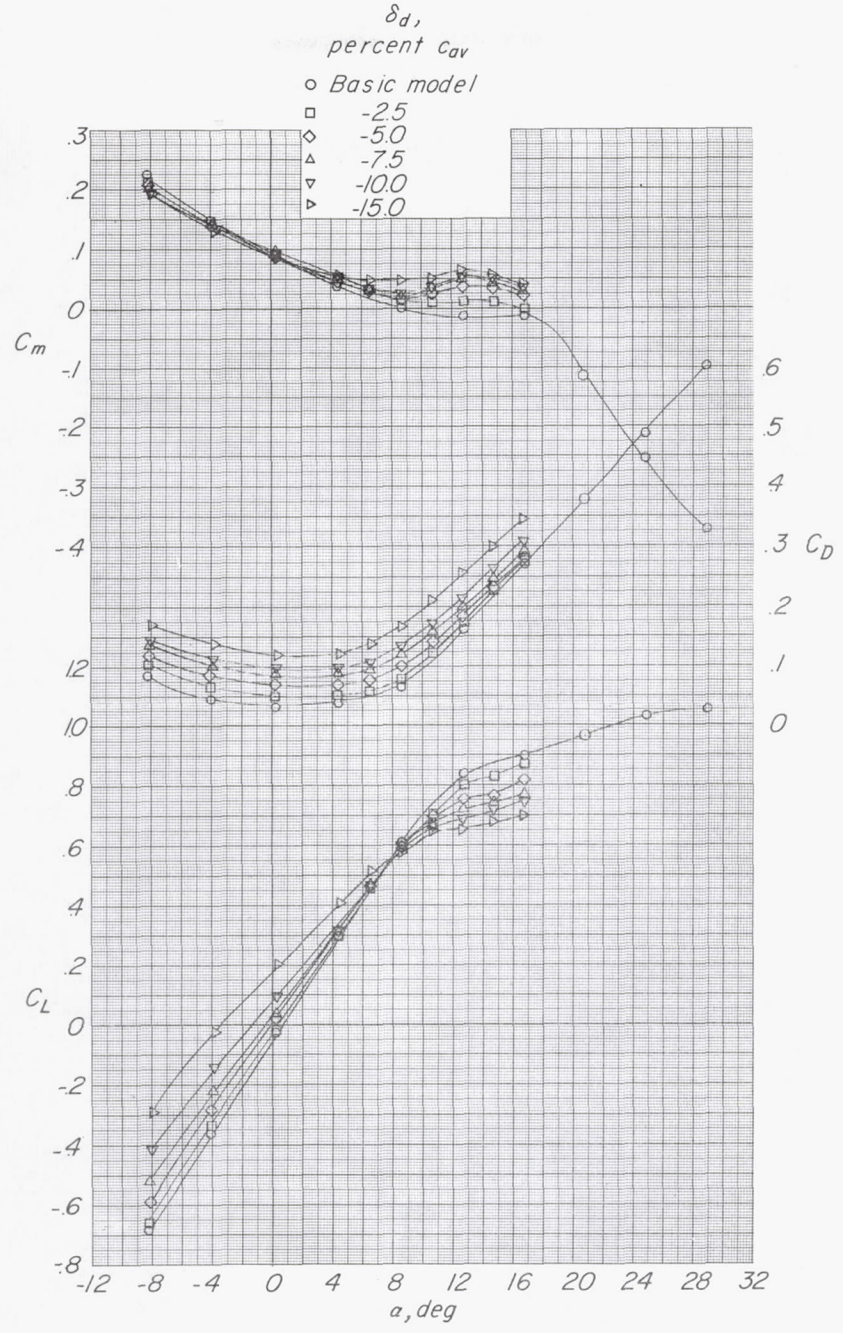

Figure 13.- Longitudinal aerodynamic characteristics of the 1/4-scale model of the X-5 airplane with deflectors. $\frac{(x_d)_{\Lambda=0^\circ}}{c_{\Lambda=0^\circ}} = 0.35$; $\frac{y_i}{b/2} = 0.34$; $\frac{y_o}{b/2} = 0.84$; $i_t = -5^\circ$.

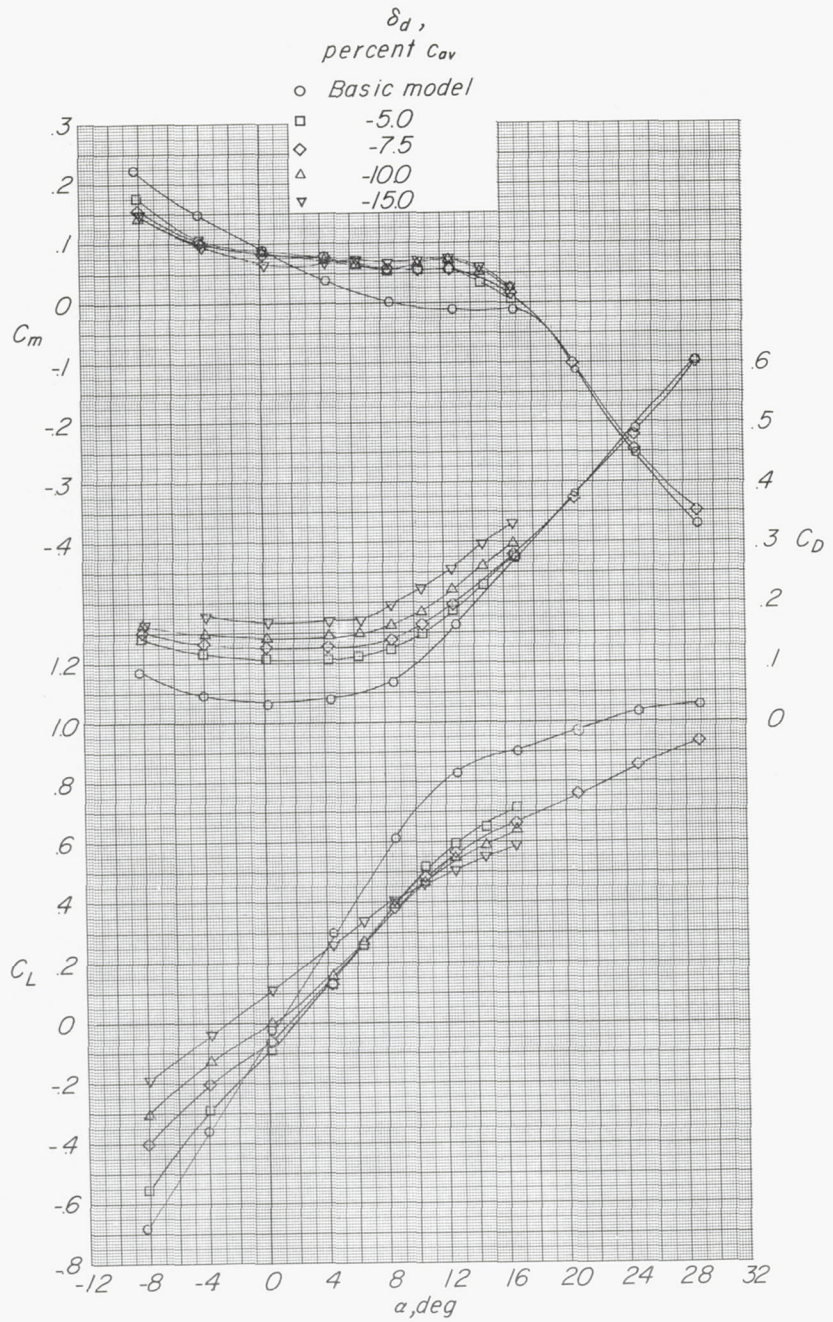

Figure 14.- Longitudinal aerodynamic characteristics of the 1/4-scale model of the X-5 airplane with a spoiler-slot-deflector. $\delta_s = -0.025c_{av}$; $\frac{(x_d)_{\Lambda=0^\circ}}{c_{\Lambda=0^\circ}} = 0.35$; $\frac{y_i}{b/2} = 0.34$; $\frac{y_o}{b/2} = 0.84$; $i_t = -5^\circ$.

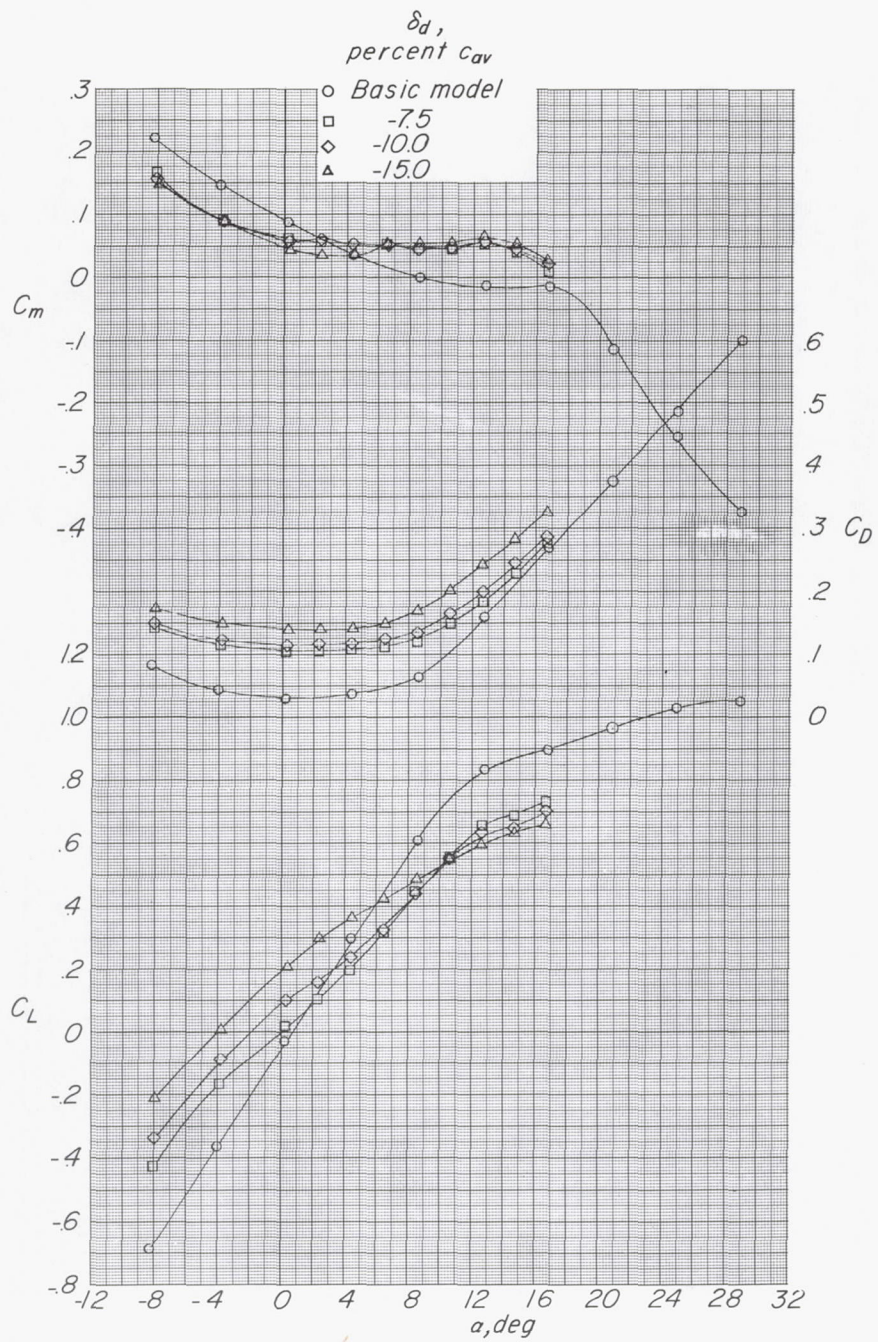

Figure 15.- Longitudinal aerodynamic characteristics of the 1/4-scale model of the X-5 airplane with slant spoiler-slot-deflector.

$\delta_s = -0.025 c_{av}$; $\frac{(x_d)_{\Lambda=0^\circ}}{c_{\Lambda=0^\circ}} = 0.35$; $\frac{y_i}{b/2} = 0.34$; $\frac{y_o}{b/2} = 0.84$; $i_t = -5^\circ$.

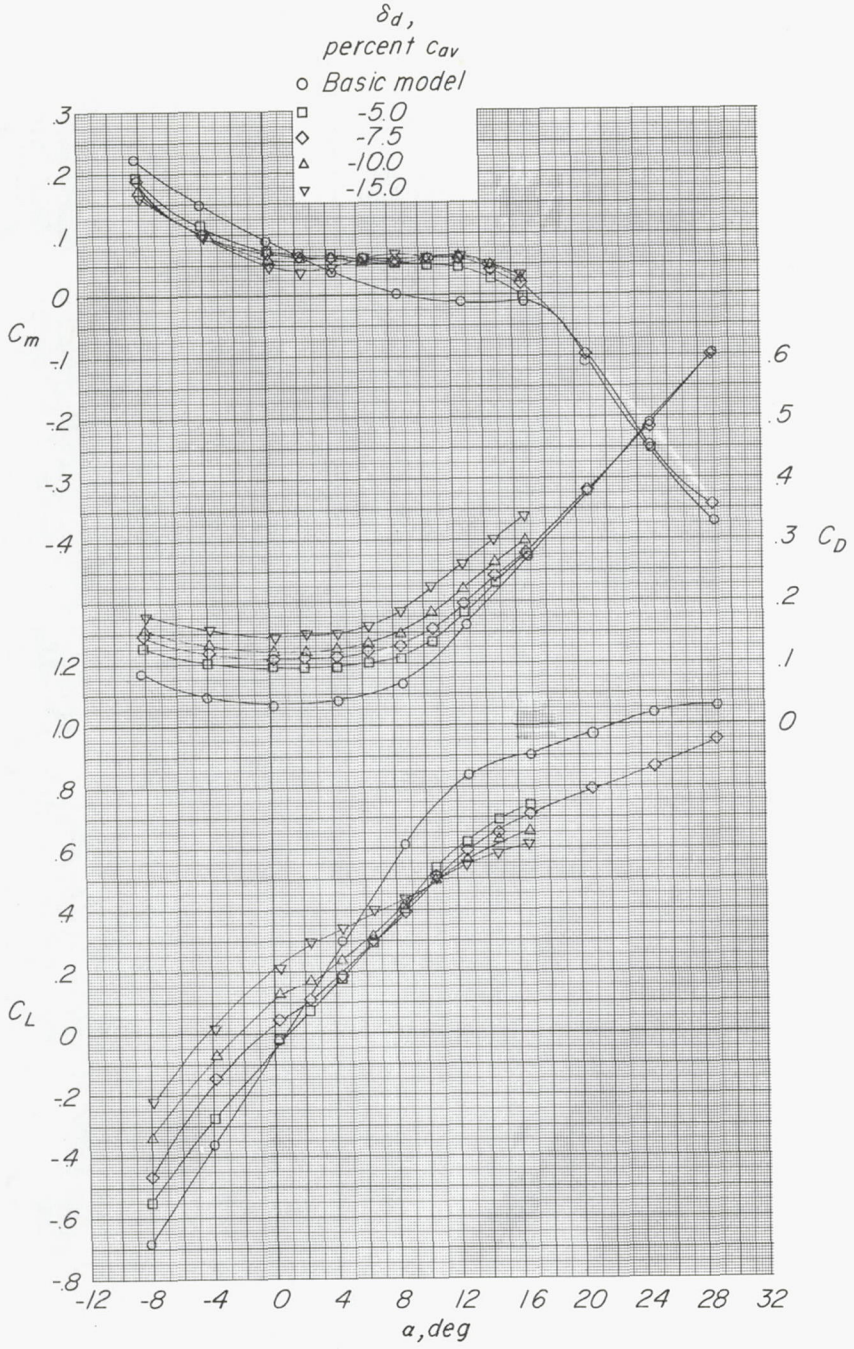

Figure 16.- Longitudinal aerodynamic characteristics of the 1/4-scale model of the X-5 airplane with a butterfly-valve arrangement.

$\delta_s = -0.025c_{av}$; $\frac{(x_d)_{\Lambda=0^\circ}}{c_{\Lambda=0^\circ}} = 0.35$; $\frac{y_i}{b/2} = 0.34$; $\frac{y_o}{b/2} = 0.84$; $i_t = -5^\circ$.

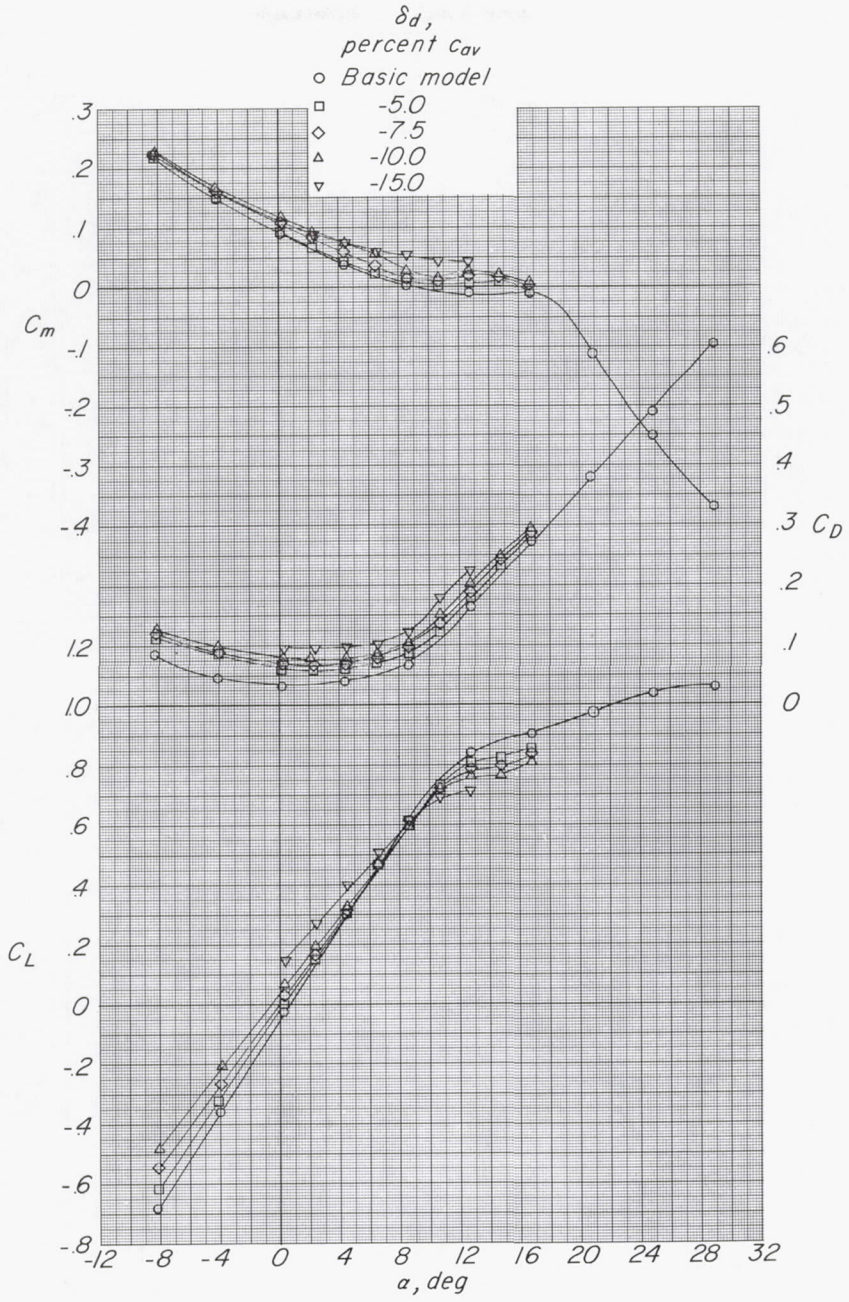

Figure 17.- Longitudinal aerodynamic characteristics of the 1/4-scale model of the X-5 airplane with deflectors. $\frac{(x_d)_{\Lambda=0^\circ}}{c_{\Lambda=0^\circ}} = 0.35$; $\frac{y_i}{b/2} = 0.34$; $\frac{y_o}{b/2} = 0.66$; $i_t = -5^\circ$.

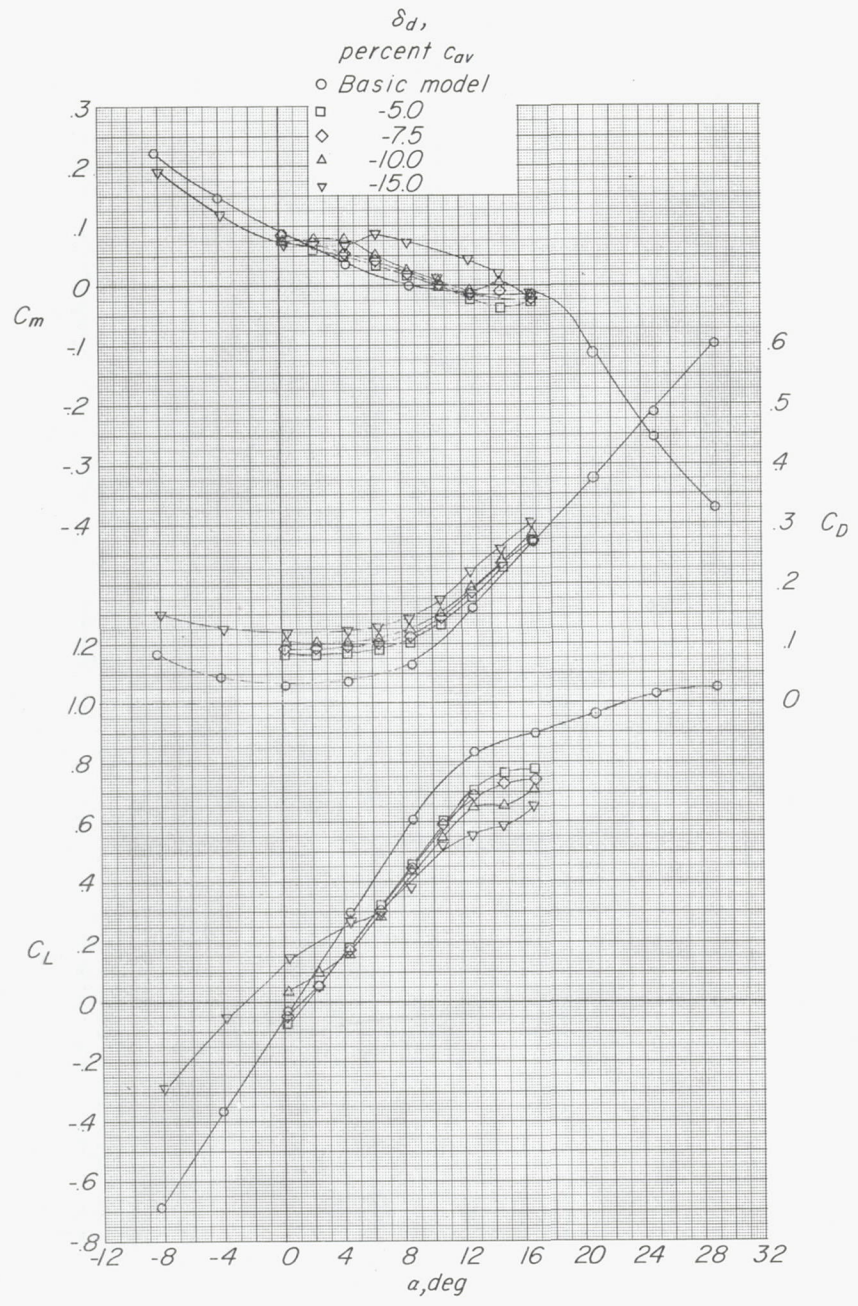

Figure 18.- Longitudinal aerodynamic characteristics of the 1/4-scale model of the X-5 airplane with a spoiler-slot-deflector. $\delta_s = -0.025c_{av}$; $\frac{(x_d)_{\Lambda=0^\circ}}{c_{\Lambda=0^\circ}} = 0.35$; $\frac{y_i}{b/2} = 0.34$; $\frac{y_o}{b/2} = 0.66$; $i_t = -5^\circ$.

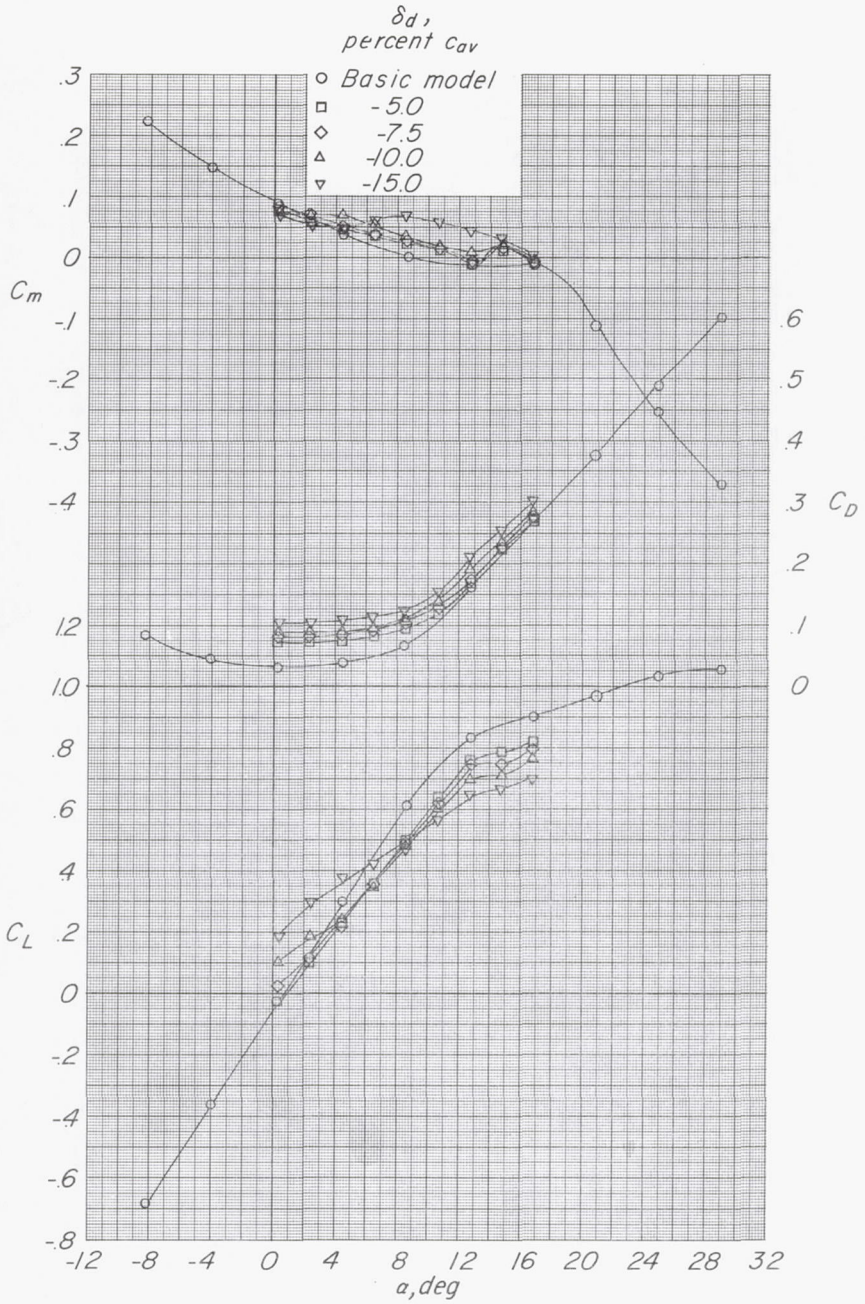

Figure 19.- Longitudinal aerodynamic characteristics of the 1/4-scale model of the X-5 airplane with slant spoiler-slot-deflector.

$\delta_s = -0.025c_{av}$; $\frac{(x_d)_{\Lambda=0^\circ}}{c_{\Lambda=0^\circ}} = 0.35$; $\frac{y_i}{b/2} = 0.34$; $\frac{y_o}{b/2} = 0.66$; $i_t = -5^\circ$.

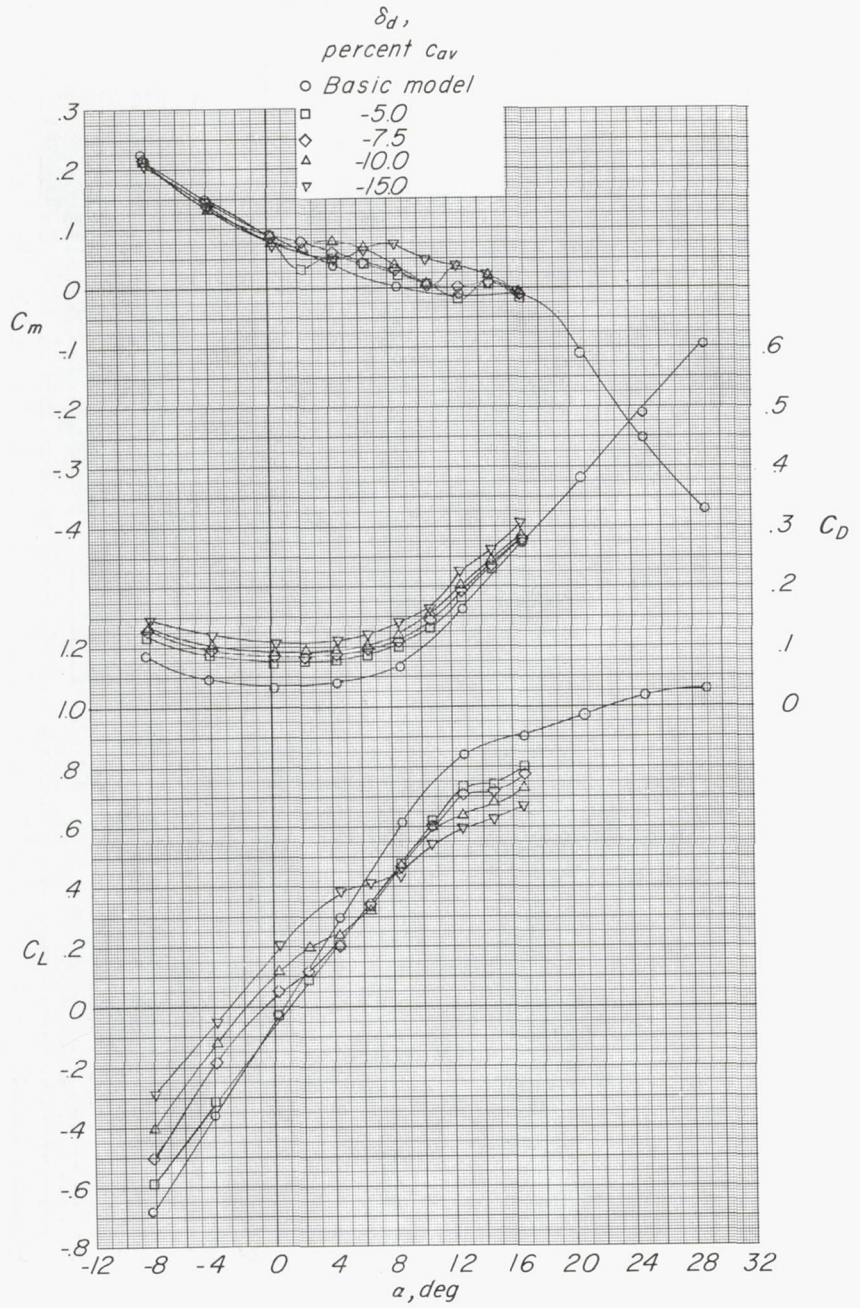

Figure 20.- Longitudinal aerodynamic characteristics of the 1/4-scale model of the X-5 airplane with butterfly-valve arrangement.

$\delta_s = -0.025c_{av}$; $\frac{(x_d)_{\Lambda=0^\circ}}{c_{\Lambda=0^\circ}} = 0.35$; $\frac{y_i}{b/2} = 0.34$; $\frac{y_o}{b/2} = 0.66$; $i_t = -5^\circ$.

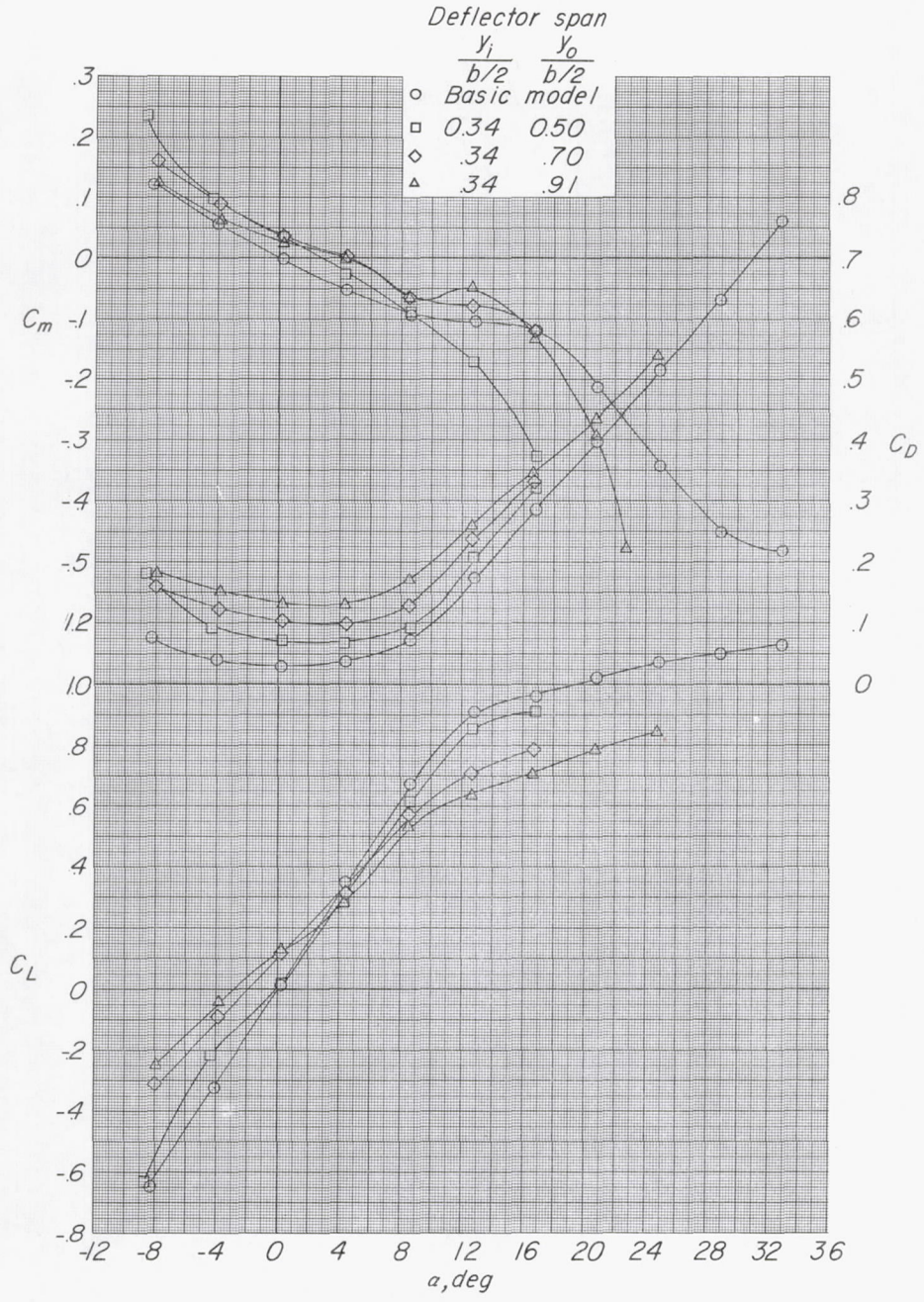

Figure 21.- Longitudinal aerodynamic characteristics of the 1/4-scale model of the X-5 airplane with deflectors. $\delta_d = -0.15c_{a.v}$; $\frac{(x_d)_{\Lambda=0^\circ}}{c_{\Lambda=0^\circ}} = 0.25$; $i_t = -3/4^\circ$.

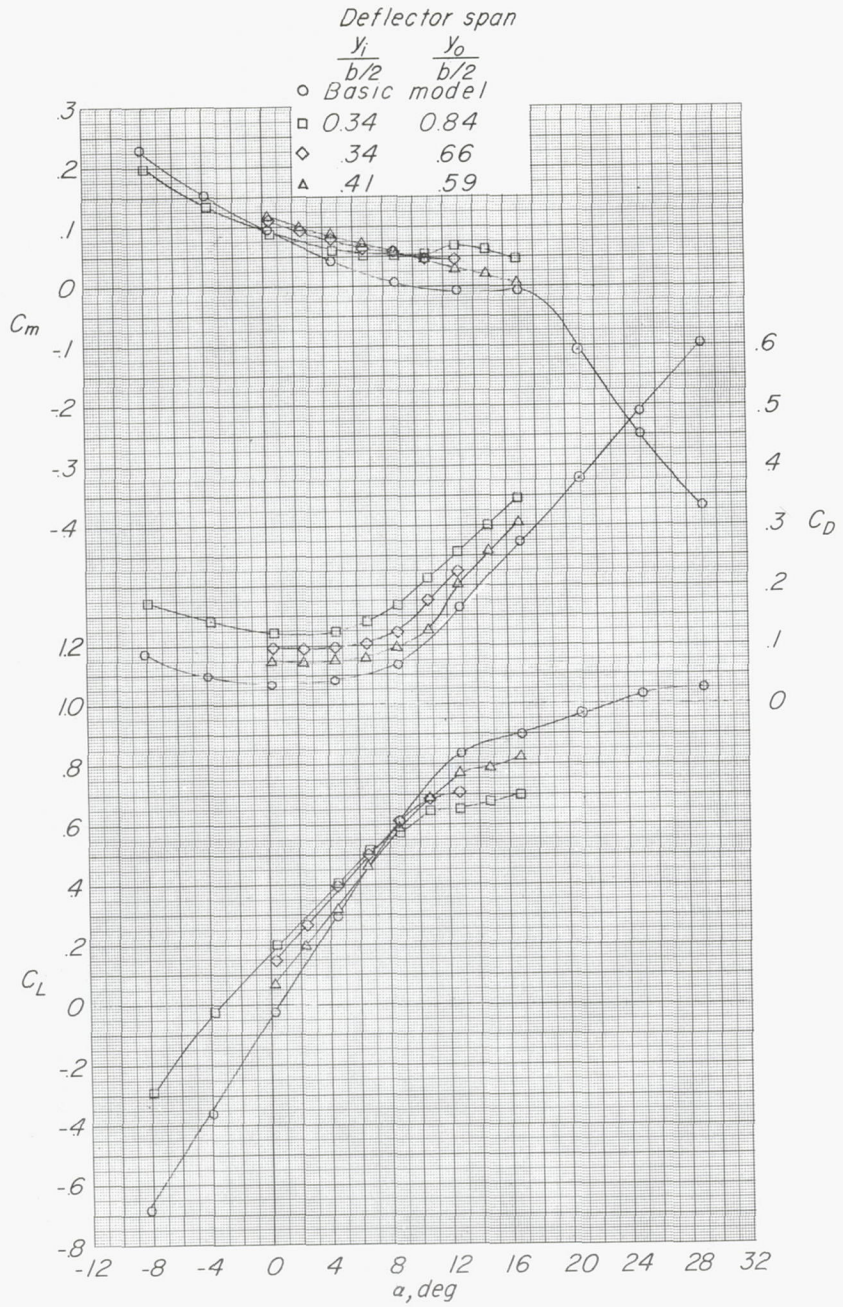

Figure 22.- Longitudinal aerodynamic characteristics of the 1/4-scale model of the X-5 airplane with deflectors. $\delta_d = -0.15c_{av}$; $\frac{(x_d)_{\Lambda=0^\circ}}{c_{\Lambda=0^\circ}} = 0.35$; $i_t = -5^\circ$.

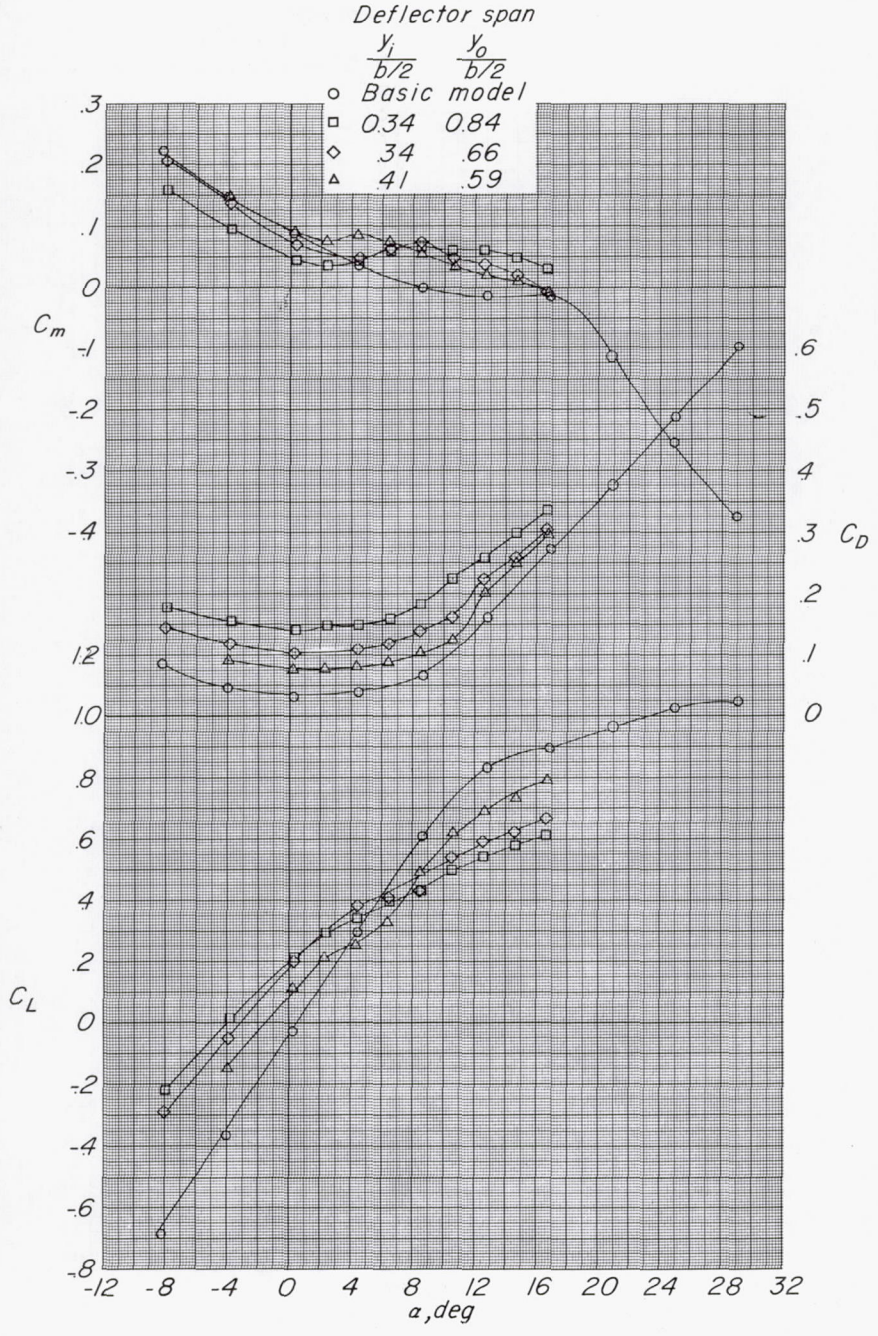

Figure 23.- Longitudinal aerodynamic characteristics of the 1/4-scale model of the X-5 airplane with a butterfly-valve arrangement.

$\delta_d = -0.15c_{av}$; $\delta_s = -0.025c_{av}$; $\frac{(x_d)_{\Lambda=0^\circ}}{c_{\Lambda=0^\circ}} = 0.35$; $i_t = -5^\circ$.

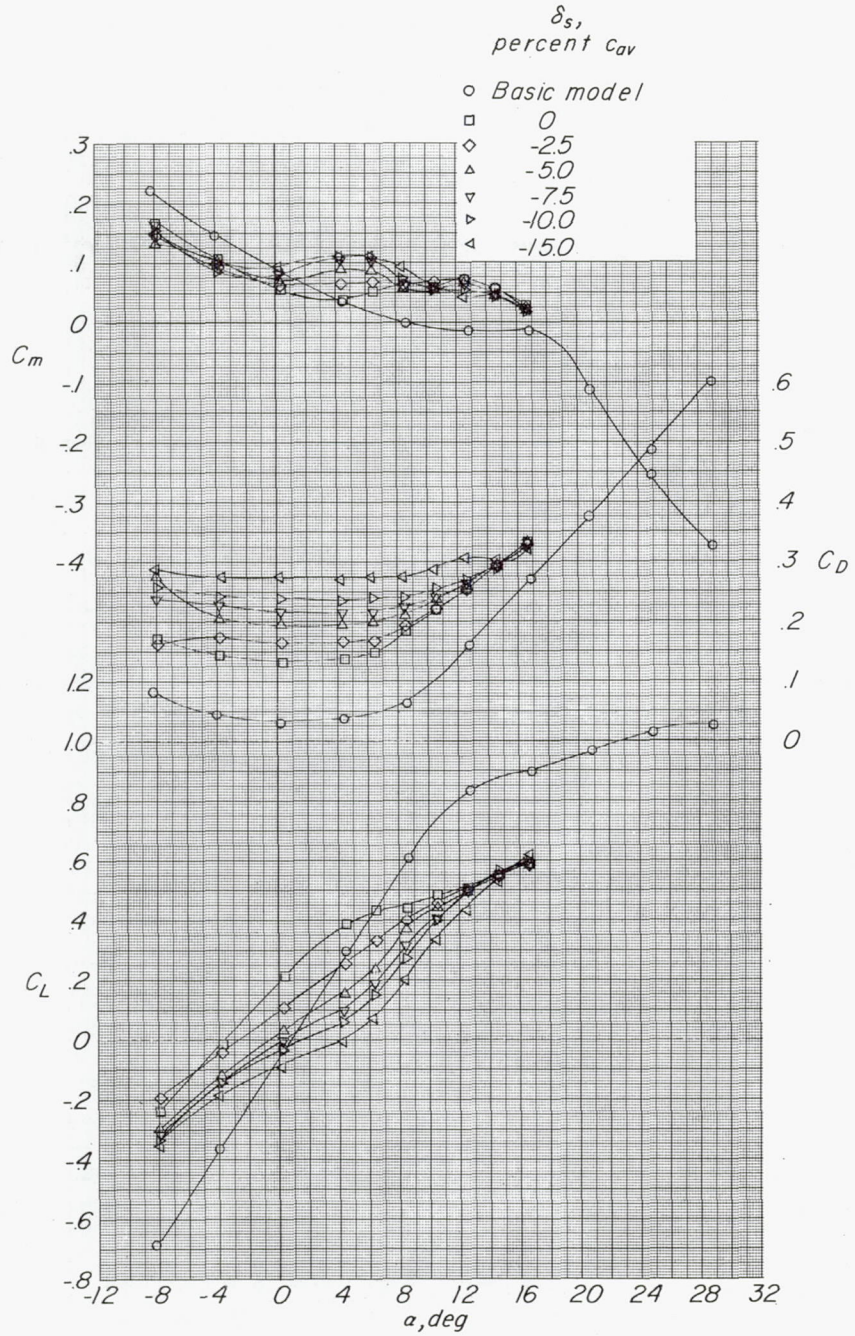

Figure 24.- Longitudinal aerodynamic characteristics of the 1/4-scale model of the X-5 airplane with spoiler-slot-deflector. $\delta_d = -0.15c_{av}$; $\frac{(x_d)_{\Lambda=0^\circ}}{c_{\Lambda=0^\circ}} = 0.35$; $\frac{y_i}{b/2} = 0.34$; $\frac{y_o}{b/2} = 0.84$; $i_t = -5^\circ$.

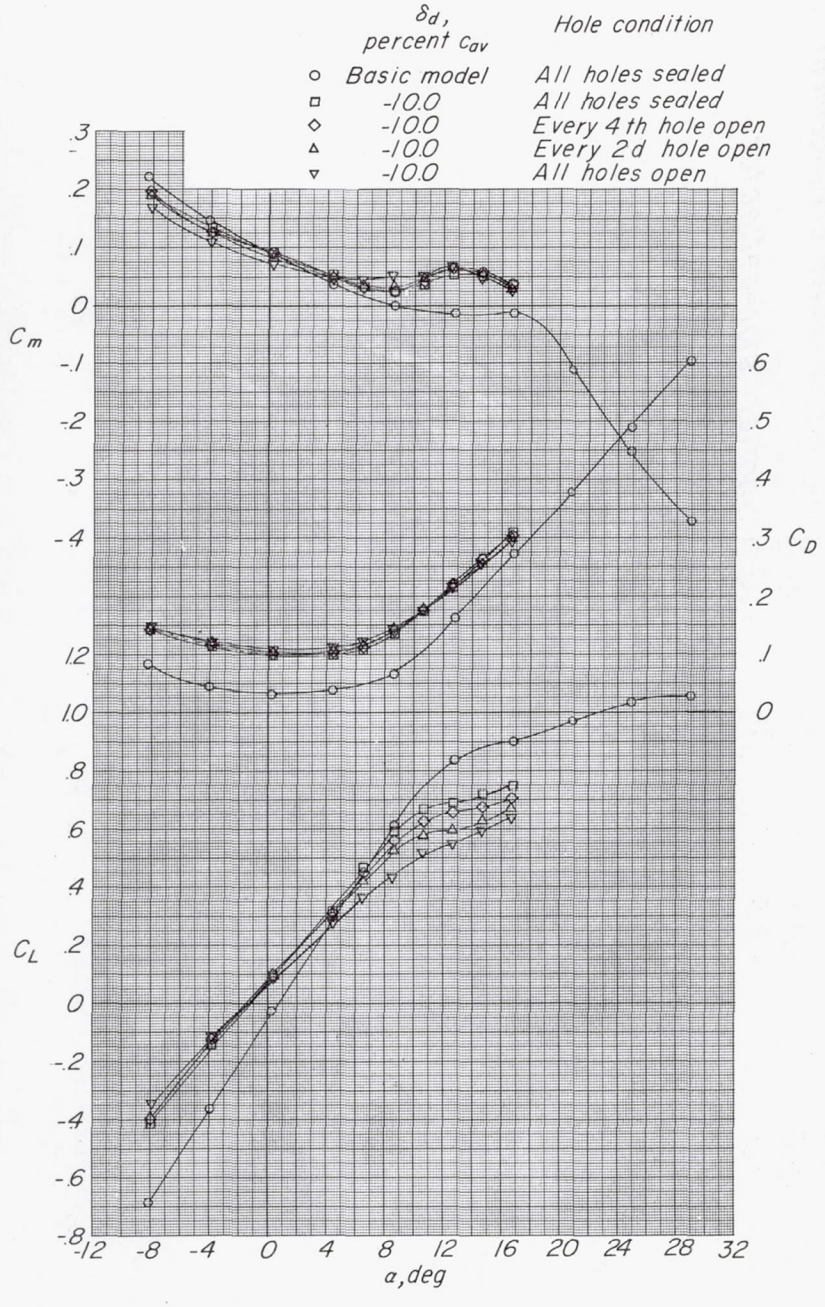

Figure 25.- Longitudinal aerodynamic characteristics of the 1/4-scale model of the X-5 airplane with various slot-deflector arrangements. $\frac{(x_d)_{\Lambda=0^\circ}}{c_{\Lambda=0^\circ}} = 0.35$; $\frac{y_i}{b/2} = 0.34$; $\frac{y_o}{b/2} = 0.84$; $i_t = -5^\circ$.

	δ_d, percent c_{av}	δ_s, percent c_{av}	$\frac{y_i}{b/2}$	$\frac{y_o}{b/2}$	
———	0	0	—	—	
— — —	-5.0	-2.5	0.34	0.84	Butterfly-valve arrangement
— - —	-5.0	-2.5	.34	.66	
— - - —	-15.0	-2.5	.34	.84	Spoiler-slot-deflector
— - - - —	-15.0	-2.5	.34	.66	

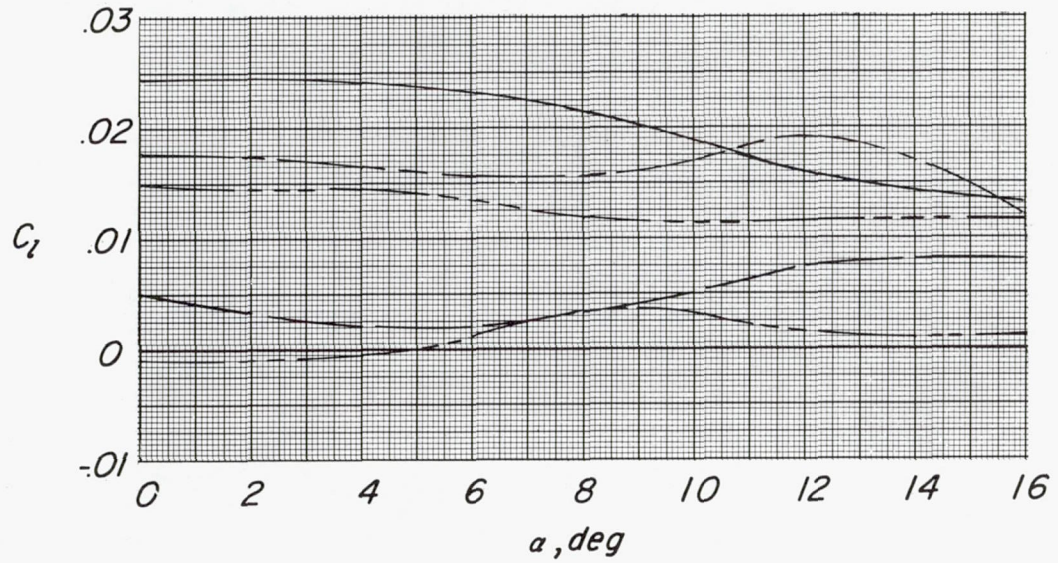

Figure 26.- Effect of span of the spoiler-slot-deflector and butterfly-valve arrangement on the aileron effectiveness for $\delta_a = \pm 10^\circ$ on the 1/4-scale model of the X-5 airplane. $\frac{(x_d)_{\Lambda=0^\circ}}{c_{\Lambda=0^\circ}} = 0.35$.

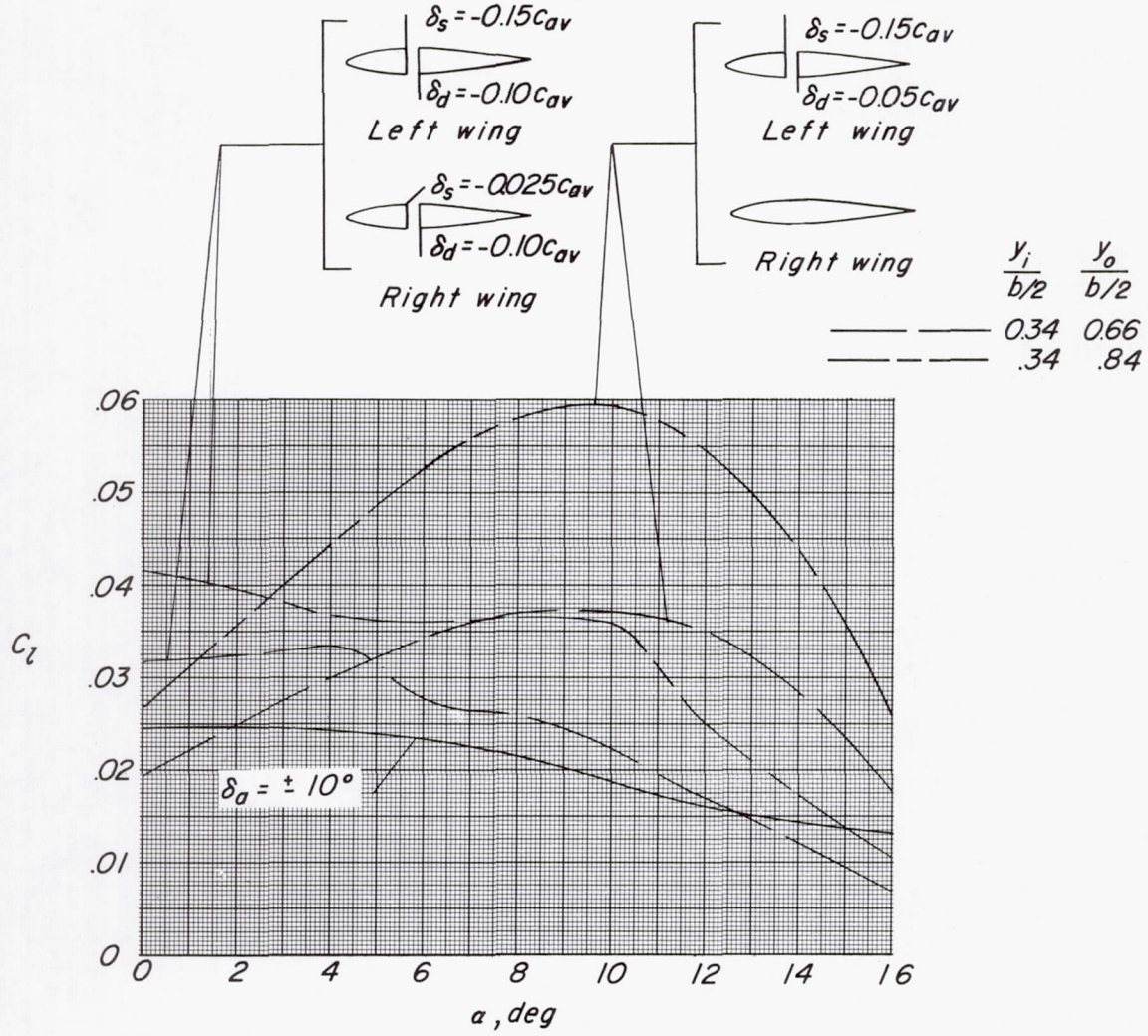

Figure 27.- Variation of rolling-moment coefficient with angle of attack for a combination gust-alleviation and lateral-control device on the 1/4-scale model of the X-5 airplane.